N4BP1 restricts HIV-1 and its inactivation by MALT1 promotes viral reactivation

Daichi Yamasoba[1,2,5], Kei Sato[3,6,7], Takuya Ichinose[1,2,5], Tomoko Imamura[2], Lennart Koepke[8], Simone Joas[8], Elisabeth Reith[8], Dominik Hotter[8], Naoko Misawa[3], Kotaro Akaki[1,2,5], Takuya Uehata[1,2], Takashi Mino[1,2], Sho Miyamoto[4], Takeshi Noda[4], Akio Yamashita[9], Daron M. Standley[10], Frank Kirchhoff[8], Daniel Sauter[8], Yoshio Koyanagi[3] and Osamu Takeuchi[1,2*]

[1]Department of Medical Chemistry, Graduate School of Medicine, [2]Laboratory of Infection and Prevention, [3]Laboratory of Systems Virology, [4]Laboratory of Ultrastructural Virology, Institute for Frontier Life and Medical Sciences, [5]Graduate School of Biostudies, Kyoto University, 53 Shogoin Kawahara-cho, Sakyo-ku, Kyoto 606-8507, Japan

[6]CREST, Japan Science and Technology Agency, Saitama 322-0012, Japan.

[7]Department of Systems Virology, Institute for Medical Science, the University of Tokyo, 4-6- 1 Shirokanedai, Minato-ku, Tokyo 108-8639, Japan

[8]Institute of Molecular Virology, Ulm University Medical Center, 89081 Ulm, Germany

[9]Department of Molecular Biology, Yokohama City University School of Medicine, Kanagawa 236-0004, Japan

[10]Department of Genome Informatics, Genome Information Research Center, Research Institute for Microbial Diseases, Osaka University, 3 Yamada-oka, Suita, Osaka 565-0871, Japan

*e-mail: otake@mfour.med.kyoto-u.ac.jp.

Abstract

RNA modulating factors not only regulate multiple steps of cellular RNA metabolism, but also emerge as key effectors of the immune response against invading viral pathogens including human immunodeficiency virus type-1 (HIV-1). However, cellular RNA binding proteins involved in the establishment and maintenance of latent HIV-1 reservoirs have not been extensively studied. Here, we screened a panel of 62 cellular RNA binding proteins and identified NEDD4 binding protein 1 (N4BP1) as potent interferon-inducible inhibitor of HIV-1 in primary T cells and macrophages. N4BP1 harbors a prototypical PIN-like RNase domain and inhibits HIV-1 replication by interacting with and degrading viral mRNA species. Upon activation of $CD4^+$ T cells, however, N4BP1 undergoes rapid cleavage at Arg509 by the paracaspase MALT1. Mutational analyses and knockout studies revealed that MALT1-mediated inactivation of N4BP1 facilitates the reactivation of latent HIV-1 proviruses. Taken together, our findings demonstrate that the RNase N4BP1 is an efficient restriction factor of HIV-1 and suggest that inactivation of N4BP1 by induction of MALT1 activation might facilitate elimination of latent HIV-1 reservoirs.

Introduction

Host cells are equipped with sophisticated mechanisms to prevent or inhibit viral infection. HIV-1 replication, for example, is targeted by a plethora of restriction factors including APOBEC3, TRIM5α, Tetherin, SAMHD1, GBP5 and MX2 [1-10]. Although these factors may suppress HIV-1 replication at various steps through multiple independent mechanisms, they are usually counteracted or evaded by the virus. Another characteristic shared by many host restriction factors is their inducibility by type I interferons (IFNs), which play a pivotal role in the host defense against viral infection [11,12].

In search of novel effective antiretroviral mechanisms, nucleic acid binding proteins are of particular interest since they are not only important regulators of antiviral gene expression, but may also act as direct effectors of the antiviral immune response [13,14]. Furthermore, they may modulate sensing of viral infection by binding to and/or degrading viral RNA or DNA species or by directly acting as pattern recognition receptors. One example of a nucleic acid-binding protein with antiviral activity is the zinc-finger antiviral protein (ZAP). Initially, ZAP was shown to degrade mouse leukemia virus (MLV) RNA by recruiting the exosome complex [15,16]. ZAP recognizes RNA sequences enriched in CG dinucleotides, which are suppressed in the genomes of HIV-1 and many other vertebrate viruses [17]. As a result, HIV-1 engineered to contain a higher number of CG dinucleotides is more sensitive to ZAP than the respective parental virus. Another example of an antiviral nucleic acid binding protein is SAMHD1. This dNTP triphosphohydrolase blocks HIV-1 reverse transcription in myeloid cells and resting T cells by depleting cellular dNTP pools [9,10,18]. Finally, the endoribonuclease Regnase-1 (also known as MCPIP1) has been suggested to degrade retroviral mRNAs [19]. Given the large number of human RNA binding proteins identified in recent studies [20,21], it seems highly likely that additional RNA binding proteins with key roles in antiviral immunity remain to be discovered. As the example of SAMHD1 illustrates [22,23], some of these

71 restriction factors might be preferentially active in resting $CD4^+$ T cells and play a role in
72 the establishment and maintenance of latent HIV-1 reservoirs.

73 To discover novel restriction factors targeting viral RNA, we screened a
74 collection of cellular proteins containing various RNA binding domains for
75 antiretroviral activity.

Results

Identification of N4BP1 as a host factor inhibiting HIV-1

To identify as-yet-unknown host restriction factors suppressing HIV-1 replication by binding to viral RNA, we selected 62 expression plasmids from mammalian gene collection (MGC) clones encoding proteins harboring at least one RNA binding domain, such as CCCH- or CCHC-type Zinc Fingers (ZF), KH domains or RNase folds (see **Supplementary Table 1**), since proteins harboring these domains may be involved in the suppression of HIV-1 [17,19]. We co-transfected HEK293T cells with the infectious HIV-1 NL4-3 molecular clone and the 62 expression plasmids, and determined infectious HIV-1 yield in the culture supernatants by infecting TZM-bl indicator cells 48 hours post-transfection. Of the 62 proteins analyzed, NEDD4 binding protein 1 (N4BP1) was the most potent inhibitor, decreasing infectious HIV-1 NL4-3 production by >20-fold (**Fig. 1a**). Immunoblot analysis of cells producing HIV-1 NL4-3 or the primary HIV-1 isolate AD17 revealed that N4BP1 expression decreased the expression of viral Env and Gag proteins in a dose-dependent manner (**Fig. 1b**). Analyzing a broader panel of primate lentiviruses, including transmitted/founder (TF) and chronic control (CC) HIV-1 strains, we found that N4BP1 reduced infectious yield of all HIV-1, HIV-2 and SIVcpz strains examined (**Fig. 1c and Supplementary Fig. 1**). Thus, N4BP1 is a broad and potent inhibitor of evolutionarily diverse primate lentiviruses.

N4BP1 is IFN-inducible and restricts HIV-1 infection in human T cells

Since antiretroviral host restriction factors are frequently inducible by IFN and virus infection, we examined if the expression of N4BP1 is IFN-inducible in T cells. IFN-α stimulation of Jurkat T cells increased N4BP1 expression at both the mRNA and protein level (**Fig. 2a and 2b**). Similarly, *N4BP1* expression was induced about 3-fold by IFN-α stimulation in $CD4^+$ T cells from healthy human donors (**Fig. 2c**). Notably, all 12 human IFN-α subtypes, but not IL-27, increased N4BP1 protein levels by about 2- to 4-fold in

primary $CD4^+$ T cells (**Supplementary Fig. 2a and 2b**). Furthermore, HIV-1 NL4-3 infection induced the expression of mRNAs encoding IFN-β, N4BP1 and the IFN-inducible proteins Tetherin/BST-2 and ISG15 in Jurkat cells (**Fig. 2d**). N4BP1 gene expression was also significantly upregulated in the spleens of HIV-1 infected humanized mice (**Fig. 2e**). Collectively, these data show that N4BP1 is a type I IFN- and HIV-1-inducible protein with potent anti-HIV-1 activity.

To determine whether endogenous N4BP1 restricts HIV-1 in human T cells, we used the CRISPR/Cas9 system to generate seven Jurkat cell lines lacking N4BP1 expression (**Fig. 2f, left panel**). HIV-1 replicated with faster kinetics in all seven *N4BP1*-deficient (KO) cell lines compared to Cas9-expressing control cells in response to HIV-1 infection (MOI 0.01) (**Fig. 2f, right panel**). Reconstitution of N4BP1 expression via a doxycycline-inducible Tet-on system (**Fig. 2g, left panel**) rescued inhibition of HIV-1 replication (**Fig. 2g, right panel**). Noteworthy, growth, apoptosis rates, or global protein synthesis were not altered between control and N4BP1 KO Jurkat cells without HIV-1 infection (**Supplementary Fig. 3a-3c**). Furthermore, N4BP1 deficiency did not affect the expression of a set of host genes such as *IFNB* and *NFKBIA* (**Supplementary Fig. 4a**). Consistently, the expression of IκBα, Tubulin-α and GAPDH proteins was not different between control and *N4BP1* KO Jurkat cells (**Supplementary Fig. 4b**), suggesting that the anti-HIV-1 effect of N4BP1 is direct and not mediated by the regulation of host genes. In agreement with the results of N4BP1 KO cells, siRNA-mediated knockdown of N4BP1 in Jurkat cells (**Supplementary Fig. 5a**) resulted in a marked increase in viral RNA expression 72 h after infection with HIV-1 NL4-3, without significantly affecting *IFNB* expression levels (**Supplementary Fig. 5b and 5c**).

Conversely, we also generated four Jurkat cell clones stably over-expressing N4BP1 or a control vector (**Fig. 2h, left panel**). N4BP1 over-expression fully prevented HIV-1 replication at low MOI (0.001) (**Fig. 2h, central panel**). Even at higher MOI (0.01), N4BP1 over-expression prevented or substantially delayed HIV-1 replication (**Fig.**

2h, right panel). Furthermore, the expression of viral RNAs including *tet*/*rev*, *vif* and *gag* was suppressed in N4BP1 over-expressing Jurkat cells (**Supplementary Fig. 5d and 5e**). These results demonstrate that N4BP1 restricts HIV-1 replication in human T cells.

Since two out of four N4BP1 overexpressing Jurkat cell clones allowed delayed but detectable replication of HIV-1 (**Fig. 2h**), we examined whether N4BP1 expression was altered in these cells following HIV-1 infection. To avoid artifacts due to differences in viral replication and spread of infection, we used an *env*-deficient (Δ*env*) VSV-G-pseudotyped HIV-1 NL4-3 construct (**Supplementary Fig. 5f**). Consistent with the results obtained with replication-competent HIV-1, production of Gag was suppressed in N4BP1 overexpressing cells compared to control cells in single cycle infection. Notably, however, N4BP1-mediated inhibition of Gag expression was less pronounced at higher MOI, suggesting that high amounts of HIV-1 may saturate the inhibitory effect of N4BP1. Furthermore, HIV-1 infection did not reduce N4BP1 expression levels (**Supplementary Fig. 5f**).

N4BP1 restricts HIV-1 in primary macrophages

IFN-α induced N4BP1 mRNA and protein expression not only in T cells (**Fig. 2a-2c**) but also in THP-1-derived macrophage-like cells (**Fig. 3a and 3b**). In addition, we found that N4BP1 is constitutively expressed in primary human monocyte-derived macrophages (MDMs) and further upregulated by IFN-α stimulation (**Fig. 3c-3e**). To examine the antiretroviral activity of N4BP1 in primary macrophages, we knocked down N4BP1 using three different siRNAs (**Fig. 3f**) before infecting the cells with the macrophage-tropic HIV-1 strain AD8. The three N4BP1-specific siRNAs increased infectious HIV-1 AD8 yield by 6.5-, 10.8- and 2.6-fold, respectively, at day 3 and by 16.2-, 14.8- and 4.3-fold by day 6 post-infection (**Fig. 3g**). Thus, N4BP1 restricts HIV-1 in both $CD4^+$ T cells and macrophages.

N4BP1 degrades HIV-1 RNA

To decipher the molecular mechanisms underlying the antiviral effect of N4BP1, we investigated whether its inhibitory activity is limited to HIV-1 and related primate lentiviruses. Overexpression of N4BP1 in HEK293T cells also inhibited MLV; genus *Gammaretrovirus*) and human foamy virus (HFV; genus *Spumavirus*) (**Fig. 4a**). However, N4BP1 failed to suppress influenza A virus mRNA expression in HEK293T cells (**Supplementary Fig. 6a**). Furthermore, N4BP1 overexpression did not reduce production of infectious influenza A virus in HEK293T cells (**Supplementary Fig. 6b**), arguing against a general and unspecific effect of N4BP1 on viral RNA expression.

Since N4BP1 reduces both HIV-1 mRNA and protein expression levels, we analyzed whether it affects proviral transcription via the long terminal repeat (LTR) using a reporter system expressing luciferase under the control of the viral LTR promoter. While NL4-3 Δ*env* induced reporter gene expression, co-expression of N4BP1 failed to suppress HIV-1 LTR-mediated gene expression (**Supplementary Fig. 7a**). In contrast, N4BP1 suppressed HIV-1 expressed under the control of the CMV promoter (pCMV259), but did not affect EGFP expression from the same promoter (**Supplementary Fig. 7b and 7c**). Together, these results suggest that N4BP1 suppresses HIV-1, but not EGFP, at a post-transcriptional level.

N4BP1 was originally identified as a target of the E3 ubiquitin ligase NEDD4, resulting in its proteasomal degradation in the nucleolus and promyelocytic leukemia (PML) bodies [24,25]. N4BP1 harbors a potential nuclease domain in addition to two KH domains, which represent canonical single-stranded nucleic acid binding domains (**Fig. 4b**) [26]. The nuclease domain of N4BP1 is highly conserved among mammalian species and structurally predicted to form a catalytic pocket with conserved aspartic acids (**Fig. 4c**). Using a subgenomic sequence of HIV-1 NL4-3 as substrate, we found that recombinant N4BP1 degrades viral RNA *in vitro* (**Fig. 4d and Supplementary Fig. 8a)**. Structural modeling of the human N4BP1 RNase domain revealed that it harbors a

catalytic center whose structure and primary amino acid sequence is similar to that of Regnase-1 (**Fig. 4e and Supplementary Fig. 8b**). A point mutation of Asp623, which is predicted to be essential part of the catalytic center, to Asn (D623N) fully abrogated the RNase activity of N4BP1 (**Fig. 4d**). Importantly, structural modeling suggests that the D623N mutation does not alter the overall structure of the RNase domain of N4BP1 (**Fig. 4e**).

Consistently, Northern blot analysis showed that N4BP1 reduces un-, singly- and multi-spliced viral mRNAs in an RNase activity-dependent manner, while ribosomal RNA was not affected (**Fig. 4f**). In contrast, incoming viral RNA was not degraded as knockdown of N4BP1 did not significantly alter the amount of early or late reverse transcriptase (RT) products or the amount of integrated proviral DNA in infected Jurkat cells (**Supplementary Fig. 8c**).

To test whether N4BP1 directly binds HIV-1 RNA, we performed an RNA immunoprecipitation (RIP) assay using the N4BP1 D623N mutant, in which the RNA-protein interaction is expected to be stable due to the lack of RNase activity. The RIP-qPCR assays revealed that the N4BP1 D623N mutant binds several HIV-1 mRNA species including splice products expressing Tat/Rev, Vif and Gag (**Fig. 4g**). In agreement with RNase-dependent restriction, wild-type N4BP1, but not the catalytically inactive mutant D623N suppressed viral protein expression (**Fig. 4h and Supplementary Fig. 8d**) and infectious HIV-1 yield (**Fig. 4i**) without affecting cell viability (**Supplementary Fig. 8e and 8f**). Collectively, these data demonstrate that N4BP1 restricts HIV-1 replication by binding and degrading viral mRNA species.

MALT1 degrades N4BP1 in T cells upon TCR-mediated activation.

Antiretroviral restriction factors are often counteracted by HIV-1 accessory proteins. N4BP1, however, inhibited wild-type HIV-1 NL4-3 and a mutant lacking all four accessory proteins (NL4-3 Δ4) with similar efficiencies (**Supplementary Fig. 9**). Thus,

we next examined N4BP1 expression levels in activated $CD4^+$ T cells that are highly permissive for HIV-1 replication and resting T cells thought to represent the main reservoir of latent HIV-1. Interestingly, N4BP1 protein levels were drastically decreased in primary $CD4^+$ T cells activated with phorbol 12-myristate 13-acetate (PMA) plus ionomycin or by treatment with anti-CD3/CD28 antibodies, but not with IFN-γ or IL-2 (**Fig. 5a**). Kinetic analysis revealed that N4BP1 levels started to decrease at 0.5 h after PMA/ionomycin stimulation and remained undetectable for at least 8 hours (**Fig. 5b**). Notably, N4BP1 mRNA levels were not markedly affected by PMA/ionomycin treatment (**Supplementary Fig. 10a**). In support of N4BP1 protein degradation, a ~72 kDa cleavage product appeared in PMA/ionomycin-treated cells (**Fig. 5b**) just above non-specific bands (65 kD and 40 kD) which is also present in N4BP1 KO cells (**Fig. 2f**). Although N4BP1 was reported to undergo NEDD4-mediated polyubiquitination [25], proteasome inhibitor treatment did not prevent PMA/ionomycin-mediated degradation of N4BP1 (**Supplementary Fig. 10b**). Further experiments revealed that PMA alone, but not ionomycin, is sufficient to decrease N4BP1 levels (**Supplementary Fig. 10c**). Similar to T cell receptor (TCR) signals, PMA activates signaling pathways via the CARMA1-BCL10-MALT1 signalosome [27]. MALT1 is known to cleave RNA binding proteins Regnase-1 and Roquin proteins[28,29]. Consistent with a previous report, overexpression of Regnase-1 also suppressed infectious HIV-1 NL4-3 production, whereas expression Roquin-1 or -2 had no inhibitory effect (**Supplementary Fig. 10d**). We therefore hypothesized that N4BP1 might also be cleaved by MALT1. Indeed, knockout of MALT1 in Jurkat cells abrogated degradation of N4BP1 in response to stimulation (**Fig. 5c**). Furthermore, the MALT1 inhibitor zVRPR-fmk, but not a pan-caspase inhibitor zVAD-fmk, suppressed cleavage of N4BP1 (**Fig. 5d**). Thus, the protease activity of MALT1 is essential for N4BP1 cleavage upon T cell activation.

MALT1 cleaves N4BP1 at R509

The appearance of a ~72 kDa cleavage product (**Fig. 5b**) suggested that the MALT1 cleavage site(s) is located in the central region of N4BP1, between the KH and RNase domains (**Fig. 5e**). Thus, we generated a series of C-terminally truncated variants to determine the exact position of the cleavage site (**Fig. 5e**). Immunoblot analysis revealed that the electrophoretic mobility of an N4BP1 mutant comprising the N-terminal 500 amino acids was close to that of MALT1 cleaved N4BP1 (**Fig. 5f**). MALT1 specifically cleaves after arginine residues [27], and analysis of previously identified MALT1 substrates revealed a putative [S/P]-R-G consensus target sequence for this protease (**Fig. 5g and Supplementary Fig. 10e**). N4BP1 harbors a highly conserved SRG motif at positions 508-510 (**Fig. 5h**), and R509A mutant N4BP1 was not cleaved by MALT1 expressed together with BCL10 (**Fig. 5i**). Furthermore, PMA/ionomycin stimulation of Jurkat cells induced cleavage of WT Flag-N4BP1, while the Flag-N4BP1 R509A mutant was resistant to cleavage (**Fig. 5j**). Notably, mutation of R509A rendered N4BP1 resistant to MALT1 cleavage without impairing its antiviral activity (**Fig. 5k**).

Degradation of N4BP1 promotes reactivation of latent HIV-1

Degradation of N4BP1 by MALT1 might be involved in the reactivation of latent HIV-1 by T cell activation. To investigate this possibility, we first examined N4BP1 expression in three different human T cell lines harboring latent HIV-1 proviruses [30-32]. N4BP1 was constitutively expressed and downmodulated upon PMA stimulation in all cell lines tested (**Supplementary Fig. 11a-c**). As expected, PMA-induced degradation of N4BP1 was abrogated in MALT1 knockout JNLGFP, J-Lat10.6 and J-Lat5A8 cells (**Fig. 6a, 6b, Supplementary Fig. 11d**). Thus, MALT1 is required for PMA-induced degradation of N4BP1 in latently HIV-1 infected T cells. MALT1-knockout JNLGFP, J-Lat10.6 and J-Lat5A8 cells showed significantly lower levels of HIV-1 reactivation than control cells in response to PMA stimulation (**Fig. 6c, 6d, and Supplementary Fig. 11e**). After

induced expression of N4BP1 in J-Lat10.6 and JNLGFP cells by a Tet-On system, wild-type but not R509A N4BP1 was degraded in response to PMA stimulation (**Fig. 6e and 6f**). Intriguingly, the MALT1-resistant N4BP1 R509A mutant suppressed the reactivation of J-Lat10.6 and JNLGFP cells more efficiently than WT N4BP1 as examined by the changes in HIV-1 p24 levels in the culture supernatants (**Fig. 6e and 6f**). We further established N4BP1 KO JNLGFP cells (**Fig. 6g**), and reconstituted them with WT N4BP1 or the R509A mutant thereof using the inducible Tet-On system (**Fig. 6h**). Consistent with the overexpression data, JNLGFP cells reconstituted with R509A N4BP1 potently suppressed reactivation of HIV-1, whereas cells reconstituted with wild-type N4BP1 failed to do so. (**Fig. 6h and 6i**). Thus, inactivation of N4BP1 by MALT1 supports latency reversal upon activation of latently HIV-1 infected T cells (**Supplementary Fig. S12**).

Discussion

Our study demonstrates that HIV-1 latency and reactivation are controlled by N4BP1 at the post-transcriptional level. Notably, two mechanisms may contribute to the maintenance of viral latency by N4BP1: First, N4BP1 generally degrades spliced- and un-spliced HIV-1 transcripts, thereby preventing their translation into viral proteins and progeny virion formation. Second, N4BP1 may continuously keep HIV-1 Tat levels below the threshold required for reactivation and efficient transcription of viral genes. Intriguingly, N4BP1 is rapidly inactivated by MALT1 in response to stimuli inducing HIV-1 reactivation, indicating that changes in MALT1 activation levels regulate HIV-1 reactivation. Thus, manipulation of MALT1 activity may be a promising approach to control HIV-1 latency and reactivation. Notably, treatment with the MALT1 inhibitor MI-2 has previously been shown to induce death of latently HIV-1 infected cells, and death rates were further increased by PMA stimulation [33]. However, specificity of MALT1 inhibition and the MALT1 targets involved in this process remained unclear. Thus, further studies are required to decipher the suitability of MALT1 as a target for therapeutic intervention.

An important open question is how N4BP1 specifically recognizes retroviral RNA, without degrading for example Influenza A virus or ribosomal RNAs. Given that multi-spliced HIV-1 RNA (encoding Tat and Rev) as well as singly or un-spliced viral mRNAs are degraded, N4BP1 might target motifs or structures in un-spliced viral mRNA, the *tat*/*rev* encoding region or end modifications found in all three mRNA classes. The frequency of CG dinucleotides is markedly suppressed in the genomes of HIV-1 as well as other vertebrate viruses, thereby attenuating ZAP-mediated restriction [17]. Given that N4BP1 suppresses various lenti- and retro-viruses including HIV-1, sequence motif(s) other than CG dinucleotides could be recognized by N4BP1.

N4BP1 is localized in the nucleus especially in the nucleolus and/or PML bodies [25]. Intriguingly, HIV-1 transcripts are specifically re-localized into nucleoli for viral gene

expression [34]. In addition, latent HIV-1 was reported to colocalize with PML bodies, with PML binding to the latent HIV-1 LTR promoter [35]. Degradation of PML led to the activation of viral transcription together with the release of histone methyltransferase G9a [35]. Given that HIV-1 RNA is suppressed by N4BP1, it is tempting to speculate that N4BP1 co-transcriptionally degrades viral mRNA in PML bodies, thereby contributing to the maintenance of latency. Although MALT1 is majorly present in the cytoplasm, this protein harbors a nuclear export signal (NES), and is reported to shuttle between nucleus and cytoplasm [36]. Thus, MALT1 might cleave N4BP1 in the nucleus.

Our data suggest that N4BP1 is not directly counteracted by HIV-1 accessory proteins. However, it is possible that HIV-1 has evolved means to evade N4BP1. Furthermore, expression of N4BP1 was diminished in T cells stimulated with PMA/ionomycin or via TCR-CD3/CD28 ligation. Considering that HIV-1 replicates efficiently in activated but not in quiescent $CD4^+$ T cells, it is tempting to speculate that reduction of N4BP1 facilitates HIV-1 replication in activated T cells. We discovered that cleavage and inactivation of N4BP1 in T cells is mediated by the protease MALT1 and identified R509 as its cleavage site. Previously described MALT1 substrates include host mRNA regulators such as Regnase-1 and Roquin. These proteins are critical for controlling immune reactions as they destabilize host mRNAs encoding proinflammatory cytokines and proteins involved in T cell activation [37,38]. It is intriguing to explore the function of N4BP1 in the control of immune responses and future studies will uncover the functional roles of N4BP1 in regulating host mRNAs *in vivo*.

A recent study determining type I interferomes of fibroblasts in multiple vertebrate species identified 62 evolutionarily conserved interferon-stimulated genes (ISGs) [12]. Interestingly, N4BP1 was also among these core ISGs. Upon IFN-α stimulation, N4BP1 suppresses HIV-1 infection by inducing its expression and/or altering its RNase activity. Additionally, the MALT1-cleavage site as well as the RNase

domain are conserved among the N4BP1 orthologs of different mammalian species, consistent with IFN-inducibility. These notions imply that the function of N4BP1 in antiviral immunity is conserved among different species. Given that human N4BP1 suppresses a variety of retroviruses, but not influenza A virus, it is tempting to speculate that N4BP1 might have an ancestral function in specifically controlling retroviral infection. Furthermore, it will be interesting to explore whether N4BP1 is involved in the post-transcriptional silencing of endogenous retroviruses.

In this study, we identified N4BP1 as a HIV-1 restriction factor by screening proteins that harbor potential RNA binding domains. As our screening approach did not include all RNA binding proteins, it is possible that additional anti-retroviral RNA binding factors remain to be discovered. Furthermore, an over-expression-based screening approach may fail to identify antiviral proteins that are endogenously expressed to high levels, if over-expression does not further increase their abundance. Therefore, further studies are required to elucidate the role of RNA binding proteins in restriction of HIV-1, e.g. by using more complete sets of RNA binding proteins and/or loss of function screening systems.

In summary, we identified N4BP1 as an RNase that functions as an antiretroviral restriction factor by degrading various HIV-1 mRNA species. Although further studies are required to precisely define the molecular mechanisms underlying target RNA recognition by N4BP1, our findings clearly demonstrate that N4BP1 is a potent effector of type I IFN-mediated anti-HIV-1 activity.

Methods

Cell culture, Proviral Constructs and Transfection.

Jurkat cells and THP-1 cells were obtained from the ATCC and grown in RPMI-1640 medium (Nacalai Tesque) supplemented with 10% fetal calf serum (FCS) and 50 μM β-mercaptoethanol (Nacali Tesque). HEK293T cells were obtained from ATCC and grown in DMEM supplemented with 10% fetal calf serum (FCS). TZM-bl cells and J-Lat10.6 cells were obtained from the NIH AIDS Research and Reference Reagent Program and maintained in DMEM medium (Nacalai tesque) supplemented with 10% fetal calf serum (FCS) or in RPMI-1640 medium (Nacalai Tesque) supplemented with 10% fetal calf serum (FCS) and 50 μM β-mercaptoethanol (Nacali Tesque) respectively. J-Lat5A8 cells were kindly provided by Warner C. Greene from the Gladstone Institute of Virology and cultured in RPMI-1640 supplemented with 10% fetal calf serum. JNLGFP cells were kindly provided by David N. Levy from the New York University College of Dentistry and cultured in RPMI1640 supplemented with 10% of FCS. Cell lines were not validated further or tested for micoplasma in our laboratory. Plasmid transfection experiments for HEK293T cells were performed using Polyethylenimine Max Mw 40000 (polysciences). Plasmid transfection experiments for Jurkat cells were performed using Neon Transfection System (Invitrogen) according to the manufacturer's protocol. HEK293T cells were transfected 24 h after seeding in 12-well plates at a confluence of 70%. Cells and supernatants were harvested 48 hours post-transfection. The pCMV-SPORT6 expression plasmids used for the screening of genes encoding proteins potentially harboring RNA binding domains listed in **Supplementary Table 1** represent verified full-length cDNA Clones (Open Biosystems) obtained through the Mammalian Gene Collection (MGC). Regnase-1 and Roquin-1 expression plasmids have been described previously [39]. The Roquin-2 expression plasmid was kindly provided by Dr. Hidenori Ichijo (The University of Tokyo). Replication competent HIV-1 particles were obtained by transfecting HEK293T cells with the following HIV-1 infectious plasmids:

pNL4-3 (cat#114) [40] was obtained through the NIH AIDS Reagent Program. HIV-1 clones pCH058 (cat#11856) [41] and pAD17 (cat#12423) [42] were obtained through the NIH AIDS Reagent Program from Dr. Beatrice Hahn (University of Pennsylvania). The SIVcpz molecular clone MB897 [43], as well as HIV-1 pCH058 (6-month), pCH077 (6-month), pCH440, pCH200v2, pCH534 and CH042 were kindly provided by Beatrice Hahn [44-46]. The HIV-1 AD8 infectious molecular clone was obtained from Cathleen Collins (UCSD, San Diego) and has been described previously [47]. The Moloney Leukemia Virus strain pMLV48 was kindly provided by Dr. Komano Atsushi (Nagoya Medical Center). The Human Foamy virus strain HSRV13 was kindly provided by David Russel (University of Washington). pCMV259 was kindly provided by Junichi Sakuragi (Osaka University)[48]. Forty eight hours post-transfection, culture supernatants were harvested, then filtrated, and stocked as a viral solution. For the replication assay, empty vector or N4BP1 expressing Jurkat cells were seeded at 2×10^5 cells in 48 well plate. Then, they were inoculated with HIV-1 NL4-3. Primary $CD4^+$ T cells were isolated from human blood from 3 healthy donors by Ficoll Paque gradient centrifugation and negative selection using the RosetteSep™ Human $CD4^+$ T cell Enrichment cocktail (Stem Cell Technologies) and cultured in RPMI1640. Monocytes were separated from PBMCs by plastic adherence and differentiated into monocyte-derived macrophages (MDM) using AB-serum (10%) and macrophage colony stimulating factor (M-CSF, R&D Systems; 15 ng/ml). Primary human macrophages were differentiated from human peripheral blood mononuclear cells from 3 healthy donors. PBMCs were seeded onto the plate in serum free RPMI-1640 for 3 hours at 37 °C. Non-adherent cells in the supernatants were discarded and adherent monocytes were cultured in RPMI-1640 with 10% FCS and M-CSF (15 ng/ml, PeproTech) for 6 days.

Generation of Virus Stocks

HEK293T cells were sown in 6-well plates and transfected with proviral HIV-1 DNA (5

μg) at a confluence of 70-80 % using a standard calcium phosphate transfection protocol. For mock infection controls, HEK293T cells were treated with transfection reagents only. Supernatants were harvested 40 h post transfection.

Infectivity Assay

Infectious HIV-1 released into the cell culture supernatant was quantified by infection of TZM-bl reporter cells. Appropriate virus dilutions were added to 5×10^3 TZM-bl cells per well of a 96-well plate. The cells were harvested 48 hours post-infection, and a β-galactosidase assay was performed using the Galacto-Star Mammalian Reporter Gene Assay System (Applied Biosystems) according to the manufacturer's protocol. Galactosidase activity was quantified as relative light units per second (RLU/s) using a 1420 ALBOSX multilabel counter (Perkin Elmer).

Plasmid Construction

The cDNA of human N4BP1 was ligated into pFlag-CMV2 (Invitrogen), pEFs-Flag-SBP, or CSII-CMV-MCS-IRES2-Bsd for mammalian cell expression. The site-directed mutant expression vectors including pFlag-CMV2 N4BP1 D623N or R509A and pEFs-Flag-SBP D623N were generated using the Quick change lighting Site-Directed Mutagenesis Kit (Agilent). Deletion mutant cDNAs encoding amino acids 1-700 (Δ1), 1-600 (Δ2), 1-500 (Δ3) and 1-400 (Δ4) of N4BP1 were inserted into the pFlag-CMV2 vector. A lentiviral packaging plasmid, CSII-CMV-MCS-IRES2-Bsd was provided by Dr. Miyoshi in Keio University. N4BP1 and its R509A mutant were inserted into the pInducer20, a Tet-on doxycycline-inducible lentiviral expression plasmid.

Immunoblotting

HEK293T cells were seeded in 12 well plates. Cell free viral solutions were pelleted by ultracentrifugation of the culture supernatants at 40, 000 rpm for 1 hour at 4°C by using

435 TL-100 (Beckman), and then lysed in the Immunoblot lysis buffer. Cell lysates were
436 mixed with 3x loading sample buffer supplemented with 15% β-mercaptoethanol. Protein
437 samples were resolved on a 5-20% NuPAGE gel (Invitrogen). Proteins were transferred
438 from the SDS-PAGE gel to Immobilon-PVDF membranes (Merck Millipore). Proteins
439 were labeled with antibodies against HIV-1 Env (1:2000; 16H3, Cat#12559, NIH AIDS
440 Research and Reference Reagent program), p24 (1:2000, polyclonal; ViroStat), Vif
441 (1:2000; #319; NIH AIDS Research and Reference Reagent program), Nef (1:2000;
442 3D12, ThermoFisher), Vpr (1:2000; 8D1, Cosmo Bio), Vpu (1:2000; #969, NIH AIDS
443 Research and Reference Reagent program), Flag (1:1000; monoclonal; F7425, Sigma, or
444 polyclonal; F7425, Sigma), Mouse IgG Isotype Control (1:1000; #31903,
445 ThermoFisher); β-Actin (1:1000; polyclonal; sc-1615, Santa Cruz), MALT1 (1:1000;
446 #2494, Cell Signaling Technology), GAPDH (1:1000; sc-47724, Santa Cruz), α-Tubulin
447 (1:1000; T9026, Sigma), IκBα (1:1000; C-21, Santa Cruz), GFP (1:1000; ab290, Abcam)
448 and N4BP1 (1:2000, ab197079, Abcam). The anti-N4BP1 antibody recognizes the
449 N-terminal portion of N4BP1 (aa 250-300).
450
451 **Drug Treatment**
452 Jurkat cells and THP-1 cells were stimulated with IFN-α (Sigma Aldrich, 1000 U/ml).
453 Jurkat cells were stimulated with 50 ng/ml Phorbol 12-myristate 13-acetate (PMA: Sigma
454 Aldrich) with or without 500 nM ionomycin (Sigma Aldrich). Human primary $CD4^+$ T
455 cells were stimulated with IFN-α subtypes (50 ng/ml) (kindly provided by Kathrin
456 Sutter, University Duisburg-Essen) or IL-27 (R&D Systems; Cat# 2526; 5 ng/ml) for 72
457 hours, IFN-γ (SIGMA Aldrich; 50 ng/ml), IL-2 (Miltenyi Biotech; 100 U/ml) or
458 anti-CD3/CD28 beads (Dynabeads Human T-Activator CD3/CD28, Gibco) for 24 hours.
459 JNLGFP, J-Lat5A8 and J-Lat10.6 cells were stimulated with 10-50 ng/ml PMA for 24
460 hours. zVRPR-fmk (Enzo Life Sciences), a MALT1 inhibitor, zVAD-fmk (R&D systems),
461 a Pan-Caspase inhibitor and MG132 (Merck Millipore),proteasome inhibitor, were used

462 at concentrations of 100 μM, 10 μM and 0.001-10 μM, respectively.

463

464 **RNA Isolation, RT and Quantitative RT-PCR**

465 Total RNA was isolated using Trizol reagent (Invitrogen). Reverse transcription was
466 performed using ReverTra Ace (TOYOBO) according to the manufacturer's instruction.
467 The relative RNA expression levels of *IFNB*, 18S, *N4BP1*, *tat/rev*, *vif*, *gag*, HIV-1 total
468 RNA, *BST2*, and *ISG15*, MLV *gag*, SIVcpz *gag*, HSRV13 *gag* and Influenza A segment 4
469 (HA) were measured by SYBR Green Real-Time PCR in Applied Biosystems Step One
470 Plus. Viral RNA in supernatants was extracted using the ZR viral RNA kit
471 (ZymoResearch). The sequences of the primers used in qPCR are shown in
472 **Supplementary Table 2**.

473

474 **Humanized Mice**

475 NOD.Cg-*Prkdc*^{scid} *Il2rg*^{tm1Sug}/Jic (NOD/SCID *Il2rg*^{null}) mice were obtained from the
476 Central Institute for Experimental Animals (Kanagawa, Japan). The mice were
477 maintained under specific-pathogen-free conditions and were handled in accordance with
478 Regulations on Animal Experimentation at Kyoto University. The study protocol was
479 approved by the Animal Experimentation Committee in Kyoto University. Human
480 $CD34^+$ hematopoietic stem cells (HSCs) were isolated from human fetal liver as
481 previously described [49]. To generate humanized mice (NOG-hCD34 mice), human fetal
482 liver-derived $CD34^+$ cells (5×10^4 to 12×10^4 cells) were intrahepatically injected into
483 newborn NOG mice aged 0 to 2 days after X-irradiation (10 cGy per mouse) in an
484 RX-650 X-ray cabinet system (Faxitron X-ray Corporation). Humanized mice were
485 randomly assigned to HIV-1 infection or mock treatment.

486

487 **Generation of N4BP1 or MALT1 Knockout Cells by the CRISPR/Cas9 System**

488 N4BP1 knockout Jurkat cells were generated by transiently transfecting

pX330-U6-Chimeric_BB-CBh-hSpCas9 plasmid (Addgene) with Neon Transfection System according to the manufacturer's protocol. N4BP1 coding exon was targeted using the following sgRNA target site: 5'- AGATATAAAAGAAACTACTG -3'. Single clones were obtained by limiting dilution in 96-well U-bottomed culture plates. Control cells were obtained following transfection of the plasmid without sgRNA. For generating MALT1 knockout Jurkat cells, cells were delivered with the sgRNA and Cas9 expressing lentivirus vector (LentiCrispr v2 puro: Addgene) targeting the MALT1 coding sequences; sgRNA1 5'-GCAGTGCATGTAAAAGATGC-3', sgRNA2 5'-ATTCAGCCAGTGGTCACAGC-3'. Control cells were obtained by transduction of lenticrispr v2 expressing non-targeting control sgRNA; 5'-GGCCGATAATGATCCGACCG -3. Two days after transduction, cells were cultured with 1μg/ml Puromycin for 10 days. Knockout of N4BP1 or MALT1 was examined by immunoblot analysis.

Establishment of Stably N4BP1 Expressing Cells

Stably N4BP1 expressing Jurkat cells were generated by transfection with CSII Bsd IRES MCS-N4BP1 using the Neon Transfection System. Three days after transfection, N4BP1 expressing cells were selected by culturing them in 10 μg/ml blasticidin-containing RPMI-1640 for 14 days. Control cells were prepared by transfecting an empty plasmid. In some experiments, single clones were obtained by limiting dilution in 96-well U-bottomed culture plates. Stably N4BP1 expressing HEK293T cells and control cells were generated by transfection with CSII Bsd IRES MCS-N4BP1 and empty plasmid, respectively. For inducible expression of N4BP1, N4BP1 KO cells, JNLGFP, N4BP1 KO JNLGFP or J-Lat10.6 cells were prepared by pseudotyped lentivirus vector transduction with pInducer20 vector with or without wild-type or R509A mutant N4BP1 followed by selection in G418.

siRNA Transfection and Infection of Macrophages and Jurkat cells

On days 7 and 10 of differentiation, MDM were transfected with N4BP1-specific or non-targeting control siRNA using Lipofectamine RNAiMAX (Life technologies) followed by infection at day 10. All siRNAs were provided in lyophilized state by ThermoFisher (#18638, #18639, #18640) or Eurofins Genomics (non-targeting control: UUCUCCGAACGUGUCCACGUdTdT) and suspended in nuclease-free water to reach a final concentration of 20 μM. siRNA transfection was performed in 12-well plates with three technical replicates for each sample. For one well, 2.25 μl siRNA were mixed with 150 μl Opti-MEM and 6 μl Lipofectamine RNAiMAX were mixed with 150 μl Opti-MEM. These two solutions were then mixed and incubated at room temperature for 10 min. Afterwards, 300 μl of the mixture was dropped on the well containing 1 ml of cell culture medium. Medium was changed 18 h after each transfection. 3 and 6 days post infection, macrophage culture supernatants were harvested and used to infect TZM-bl reporter cells. To this end, 6,000 TZM-bl cells were sown in 96-well plates and infected in triplicate with cell culture supernatants containing infectious virus. Three days later, infection rates were determined using a galactosidase screen kit (GalScreen-Applied Bioscience) according to the manufacturer's instructions. β-galactosidase activities were quantified as relative light units per second (RLU/s) using an Orion Microplate Luminometer. For knockdown in Jurkat cells, cells were transfected with N4BP1-specific siRNA (s18640) or negative control siRNA using NEON according to the manufacturer's protocol. Differentiated human macrophages were transfected with siRNA on days 6 and 8 after isolation. Cells were transfected with N4BP1-specific siRNA (s18638-18640) or negative control siRNA using Lipofectamin RNAiMAX (Life technologies) according to the manufacturer's instructions.

Structure Modeling.

The PIN RNase domain of human N4BP1 was modeled with the SFAS threading meta

server (http://sysimm.ifrec.osaka-u.ac.jp/sfas2/) using human Regnase-1 (PDB Identifier 3v32, chain B) as a template. The conservation heatmap was constructed by aligning the top 1000 hits from the NCBI nr database to human N4BP1 using MAFFT (PMID: 23329690), and computing the sequence identity to human N4BP1. The sequence identity was expressed as a temperature factor in the human N4BP1 model PDB file and displayed in PyMOL (The PyMOL Molecular Graphics System, Version 1.8 Schrödinger, LLC.).

Generation of Recombinant N4BP1 and N4BP1-D623N Proteins

HEK293T cells were transfected with pEFs_Flag-SBP-N4BP1 or pEFs_Flag-SBP-N4BP1-D623N using polyethyleneimine "MAX" (Polysciences). Three days after transfection, cells were lysed in NF-lysis buffer [20 mM Tris (pH 7.5), 150 mM NaCl, 0.25 M Sucrose, 0.5% (v/v) NP-40, 1% (v/v) Tween 20] containing 1 mM DTT, protease inhibitor cocktail (Nacalai Tesque), phosphatase inhibitor cocktail (EDTA free) (Nacalai Tesque) and 50 μg/ml RNase A. SBP-tagged proteins were captured by Streptavidin Mag Sepharose (GE Healthcare) and eluted with T buffer (20 mM HEPES (pH 7.5), 150 mM NaCl, 2.5 mM $MgCl_2$, 0.05% (v/v) Tween 20) containing 1 mM DTT, 0.1 x protease inhibitor cocktail (EDTA free) (Nacalai Tesque), 0.1 x phosphatase inhibitor cocktail (Nacalai Tesque) and 2 mM d-desthiobiotin (Sigma-Aldrich).

***In vitro* RNA Cleavage Assay**

The *in vitro* RNA cleavage assay has been previously described [39]. Briefly, recombinant N4BP1 protein and *in vitro* transcribed 5′-[^{32}P]-labelled viral RNA (*tat*, *rev* and *nef* subgenomic RNA of HIV-1 NL4-3) [50] or a 513 base RNA fragment from the pBluescript® vector) were mixed in cleavage buffer (25 mM HEPES, 50 mM potassium acetate, 5 mM DTT, 5 mM magnesium acetate and 0.2 U/ml RNasin (Promega)) for 60 min at 37 degrees. The cleaved RNA was analyzed by denaturing 6% polyacrylamide-TBE-urea gels (Invitrogen) and autoradiography. The sequence used for

in vitro transcription and the *in vitro* cleavage assay is shown in **Supplementary Table 3**.

Northern Blotting.

Using Trizol reagent, total RNA was isolated from HEK293T cells 48 hours post-transfection with pNL4-3 together with N4BP1 expression plasmid, D623N or empty plasmid. Extracted RNA was electrophoretically separated, transferred to Hybond-N+ (GE healthcare), and hybridized with the probe derived from a fragment of pNL4-3. ^{32}P-labeled probe was generated from the 422-nt XhoI/BamHI restriction fragment in the 3' UTR of pNL4-3, which is present in all HIV-1 mRNAs. HIV-1 primary RNA transcripts, generated by alternative splicing, were detected as three major bands representing three different sizes.

RNA-Immunoprecipitation and qPCR Analysis

HEK293T cells seeded at 3×10^6 in 10 cm plates were transfected with 5 μg of pNL4-3 together with 5 μg of a plasmid expressing the N4BP1 D623N mutant. Flag-tagged N4BP1 was immunoprecipitated with an anti-Flag antibody (Sigma) or control mouse IgG isotype controls (Thermo Fisher) 48 hours after transfection. N4BP1 interacting HIV-1 RNA was extracted using Trizol, quantified by RT-qPCR and normalized to 18S RNA bound in a non-specific manner.

Analysis of Global Protein Synthesis

Control and N4BP1 KO Jurkat cells were cultured for 1 day. As negative control, some control cells were treated with a protein synthesis inhibitor, Cycloheximide (Cayman Chemical) for 30 min. Then the cells were harvested, and translating polypeptides were labeled with O-Propargyl-Puromycin (OPP) for 30 min at 37 °C followed by staining with 5 FAM Azide using the Protein Synthesis Assay kit (Cayman Chemical) according to the manufacturer's instruction. The cells were analyzed by Flow cytometry

(FACSVerse; BD). The data analysis was performed using FlowJo (LCC).

HIV-LTR Reporter Gene Assay.

TZM-bl cells cells were transfected with pGL3-HIV-LTR-Luc plasmid or pGL3-empty plasmid together with N4BP1 expression plasmid or empty control plasmid. 24 h post-transfection, cells were lysed and luciferase activities in the lysates were determined using the Dual-luciferase reporter assay system (Promega).

Detection of Early RT products, Late RT product and Integrated Proviral DNA

Quantification of HIV-1 early RT (R/U5), late RT (U5/*gag*) and integrated products by real-time PCR was done by following a published protocol (Suzuki et al., 2003). Briefly, virus was treated with DNase-I (TAKARA) at a concentration of 20 mg/ml in the presence of 10mM $MgCl_2$ at the room temperature. Heat-inactivated (65°C, 30 min) virus was used as a negative control for infection. Jurkat cells were transfected with N4BP1 or control siRNA. One day after transfection, Jurkat cells were exposed to HIV-1 NL4-3 (MOI 0.1) or heat inactivated HIV-1 at 37°C for 2 hours. Total DNA was isolated 12 hours after infection, by using DNeasy Blood & Tissue Kits (QIAGEN) according to the manufacturer's instructions. Early RT products, late RT products and integrated DNA were quantified by real-time PCR as described previously (Suzuki et al., 2003).

Influenza Infection Experiment

HEK293T cells stably expressing N4BP1 or control plasmid were infected with Influenza A virus PR8 or WSN strain for 24 hours before total RNA or culture media were harvested. Total RNA was subjected to qPCR analysis to measure the expression levels of viral mRNA for segment 4 (HA). The viral growth in the culture media was titrated by using plaque assays on Madin–Darby canine kidney (MDCK) cells.

624

625 **Statistical Analysis and Reproducibility.**

626 Statistical analyses were conducted using Prism 8 (GraphPad, La Jolla, CA, USA) or
627 Excel for Office365. Statistical significance was calculated with an unpaired two-tailed
628 Student's *t*-test. Data are presented as the mean ± s.d.. A P value of < 0.05 was considered
629 statistically significant. The screening of RBPs restricting HIV-1 was repeated and the
630 results were confirmed in an independent experiment (Fig. 1a). The *in vivo* experiment
631 with humanized mice (Fig. 2e) was performed once. The data for HIV-1 yield in MDM
632 treated with N4BP1-specific siRNAs (Fig. 3g) and p24 production comparing between
633 WT or R509A mutant N4BP1 reconstituted JNLGFP cells (Fig. 6h) are pooled from
634 three independent experiments. Other *In vitro* experiments were representative of 2-5
635 independent experiments with similar results.

636

637 **Data Availability**

638 The data that support the findings of this study are available from the corresponding
639 author upon request.

640

641

642

Acknowledgements

We thank all colleagues in our laboratory for helpful discussion, M. Tsuji and J. Hasegawa for secretarial assistance, as well as R. Linsenmeyer and J. A. van der Merwe for excellent technical assistance. We thank Kathrin Sutter (University of Duisburg-Essen, Germany) for providing IFNα subtypes and Cathleen Collins (UCSD, USA), Beatrice Hahn (University of Pennsylvania, USA), Warner C. Greene (Gladstone Institute for Virology and immunology, USA), David N. Levy (New York University of Dentistry), Hung Fan (UC Irvine, USA) and David Russell (University of Washington, USA) for providing plasmids. This work was supported by the Agency for Medical Research and Development (AMED) under Grant Numbers JP16gm0410017 (to O.T.), 18fk0410014h0001 (to O.T.), JP18fm0208006h002 (to K.S.), JP18fk0410019h0001 (to K.S.) and JP18fk0410014h0001 (to Y.K.); the Japan Society for the Promotion of Science (JSPS) KAKENHI Grant Number 18H05278 (to O.T.), 16H06429 (to K.S.), 16K21723 (to K.S.), and 17H05813 (to K.S.), and 18H02662 (to K.S.), Joint Usage/Research Center Program of Institute for Frontier Life and Medical Sciences Kyoto University (to O.T., K.S. and Y.K.); and Core-to-Core Program. This work was also supported by grants from Takeda Science Foundation and The Uehara Memorial Foundation (to O.T.). D.S. was supported by the DFG priority program “Innate Sensing and Restriction of Retroviruses” (SPP 1923) and the junior professorship programme of the state Baden-Wuerttemberg. FK is also supported by SPP 1923, DFG CRC 1279 and an Advanced ERC grant (Anti-Virome).

Author Contributions

D.Y., K.S., D.S. and O.T. designed the study. D.Y. designed, carried out and analyzed experiments. T.I., T.I., L.K., S.J., E.R., D.H., N.M, K.A, T.U and T.M. provided technical and intellectual assistance. S.M. and T.N. conducted influenza infection experiments. A.Y. provided recombinant proteins. D.S. performed structural modeling

and bioinformatic analysis. D.Y., D.S. and O.T. wrote the manuscript. K.S, F.K., Y.K. and O.T. supervised the study.

Competing interests

The authors declare no competing financial interests.

References

1 Simon, V., Bloch, N. & Landau, N. R. Intrinsic host restrictions to HIV-1 and mechanisms of viral escape. *Nat Immunol* **16**, 546-553, doi:10.1038/ni.3156 (2015).

2 Krapp, C. *et al.* Guanylate Binding Protein (GBP) 5 Is an Interferon-Inducible Inhibitor of HIV-1 Infectivity. *Cell Host Microbe* **19**, 504-514, doi:10.1016/j.chom.2016.02.019 (2016).

3 Goujon, C. *et al.* Human MX2 is an interferon-induced post-entry inhibitor of HIV-1 infection. *Nature* **502**, 559-562, doi:10.1038/nature12542 (2013).

4 Kane, M. *et al.* MX2 is an interferon-induced inhibitor of HIV-1 infection. *Nature* **502**, 563-566, doi:10.1038/nature12653 (2013).

5 Liu, Z. *et al.* The interferon-inducible MxB protein inhibits HIV-1 infection. *Cell Host Microbe* **14**, 398-410, doi:10.1016/j.chom.2013.08.015 (2013).

6 Stremlau, M. *et al.* The cytoplasmic body component TRIM5alpha restricts HIV-1 infection in Old World monkeys. *Nature* **427**, 848-853, doi:10.1038/nature02343 (2004).

7 Neil, S. J., Zang, T. & Bieniasz, P. D. Tetherin inhibits retrovirus release and is antagonized by HIV-1 Vpu. *Nature* **451**, 425-430, doi:10.1038/nature06553 (2008).

8 Van Damme, N. *et al.* The interferon-induced protein BST-2 restricts HIV-1 release and is downregulated from the cell surface by the viral Vpu protein. *Cell Host Microbe* **3**, 245-252, doi:10.1016/j.chom.2008.03.001 (2008).

9 Hrecka, K. *et al.* Vpx relieves inhibition of HIV-1 infection of macrophages mediated by the SAMHD1 protein. *Nature* **474**, 658-661, doi:10.1038/nature10195 (2011).

10 Laguette, N. *et al.* SAMHD1 is the dendritic- and myeloid-cell-specific HIV-1 restriction factor counteracted by Vpx. *Nature* **474**, 654-657, doi:10.1038/nature10117 (2011).

11 Doyle, T., Goujon, C. & Malim, M. H. HIV-1 and interferons: who's interfering with whom? *Nat Rev Microbiol* **13**, 403-413, doi:10.1038/nrmicro3449 (2015).

12 Shaw, A. E. *et al.* Fundamental properties of the mammalian innate immune system revealed by multispecies comparison of type I interferon responses. *PLoS Biol* **15**, e2004086, doi:10.1371/journal.pbio.2004086 (2017).

13 Carpenter, S., Ricci, E. P., Mercier, B. C., Moore, M. J. & Fitzgerald, K. A. Post-transcriptional regulation of gene expression in innate immunity. *Nat Rev Immunol* **14**, 361-376, doi:10.1038/nri3682 (2014).

14 Mino, T. & Takeuchi, O. Post-transcriptional regulation of cytokine mRNA controls the initiation and resolution of inflammation. *Biotechnol Genet Eng Rev* **29**, 49-60, doi:10.1080/02648725.2013.801236 (2013).

15 Gao, G., Guo, X. & Goff, S. P. Inhibition of retroviral RNA production by ZAP, a CCCH-type zinc finger protein. *Science* **297**, 1703-1706, doi:10.1126/science.1074276 (2002).

16 Zhu, Y. *et al.* Zinc-finger antiviral protein inhibits HIV-1 infection by selectively targeting multiply spliced viral mRNAs for degradation. *Proc Natl Acad Sci U S A* **108**, 15834-15839, doi:10.1073/pnas.1101676108 (2011).

17 Takata, M. A. *et al.* CG dinucleotide suppression enables antiviral defence targeting non-self RNA. *Nature* **550**, 124-127, doi:10.1038/nature24039 (2017).

18 Goldstone, D. C. *et al.* HIV-1 restriction factor SAMHD1 is a deoxynucleoside triphosphate triphosphohydrolase. *Nature* **480**, 379-382, doi:10.1038/nature10623 (2011).

19 Liu, S. *et al.* MCPIP1 restricts HIV infection and is rapidly degraded in activated CD4+ T cells. *Proc Natl Acad Sci U S A* **110**, 19083-19088, doi:10.1073/pnas.1316208110 (2013).

20 Gerstberger, S., Hafner, M. & Tuschl, T. A census of human RNA-binding proteins. *Nat Rev Genet* **15**, 829-845, doi:10.1038/nrg3813 (2014).

21 Castello, A. *et al.* Insights into RNA Biology from an Atlas of Mammalian mRNA-Binding Proteins. *Cell* **149**, 1393-1406, doi:10.1016/j.cell.2012.04.031 (2012).

22 Baldauf, H. M. *et al.* SAMHD1 restricts HIV-1 infection in resting CD4(+) T cells. *Nat Med* **18**, 1682-1687, doi:10.1038/nm.2964 (2012).

23 Descours, B. *et al.* SAMHD1 restricts HIV-1 reverse transcription in quiescent CD4(+) T-cells. *Retrovirology* **9**, 87, doi:10.1186/1742-4690-9-87 (2012).

24 Murillas, R., Simms, K. S., Hatakeyama, S., Weissman, A. M. & Kuehn, M. R. Identification of developmentally expressed proteins that functionally interact with Nedd4 ubiquitin ligase. *J Biol Chem* **277**, 2897-2907, doi:10.1074/jbc.M110047200 (2002).

25 Sharma, P., Murillas, R., Zhang, H. & Kuehn, M. R. N4BP1 is a newly identified nucleolar protein that undergoes SUMO-regulated polyubiquitylation and proteasomal turnover at promyelocytic leukemia nuclear bodies. *J Cell Sci* **123**, 1227-1234, doi:10.1242/jcs.060160 (2010).

26 Marco, A. & Marin, I. CGIN1: a retroviral contribution to mammalian genomes. *Mol Biol Evol* **26**, 2167-2170, doi:10.1093/molbev/msp127 (2009).

27 Thome, M. Multifunctional roles for MALT1 in T-cell activation. *Nat Rev Immunol* **8**, 495-500, doi:10.1038/nri2338 (2008).

28 Uehata, T. *et al.* Malt1-induced cleavage of regnase-1 in CD4(+) helper T cells regulates immune activation. *Cell* **153**, 1036-1049, doi:10.1016/j.cell.2013.04.034

(2013).

29 Jeltsch, K. M. *et al.* Cleavage of roquin and regnase-1 by the paracaspase MALT1 releases their cooperatively repressed targets to promote T(H)17 differentiation. *Nat Immunol* **15**, 1079-1089, doi:10.1038/ni.3008 (2014).

30 Jordan, A., Bisgrove, D. & Verdin, E. HIV reproducibly establishes a latent infection after acute infection of T cells in vitro. *EMBO J* **22**, 1868-1877, doi:10.1093/emboj/cdg188 (2003).

31 Kutsch, O., Benveniste, E. N., Shaw, G. M. & Levy, D. N. Direct and quantitative single-cell analysis of human immunodeficiency virus type 1 reactivation from latency. *J Virol* **76**, 8776-8786 (2002).

32 Chan, J. K., Bhattacharyya, D., Lassen, K. G., Ruelas, D. & Greene, W. C. Calcium/calcineurin synergizes with prostratin to promote NF-kappaB dependent activation of latent HIV. *PLoS One* **8**, e77749, doi:10.1371/journal.pone.0077749 (2013).

33 Li, H., He, H., Gong, L., Fu, M. & Wang, T. T. Short Communication: Preferential Killing of HIV Latently Infected CD4(+) T Cells by MALT1 Inhibitor. *AIDS Res Hum Retroviruses* **32**, 174-177, doi:10.1089/AID.2015.0343 (2016).

34 Michienzi, A., Cagnon, L., Bahner, I. & Rossi, J. J. Ribozyme-mediated inhibition of HIV 1 suggests nucleolar trafficking of HIV-1 RNA. *Proc Natl Acad Sci U S A* **97**, 8955-8960 (2000).

35 Lusic, M. *et al.* Proximity to PML Nuclear Bodies Regulates HIV-1 Latency in CD4+T Cells. *Cell Host & Microbe* **13**, 665-677, doi:10.1016/j.chom.2013.05.006 (2013).

36 Nakagawa, M. *et al.* MALT1 contains nuclear export signals and regulates cytoplasmic localization of BCL10. *Blood* **106**, 4210-4216, doi:10.1182/blood-2004-12-4785 (2005).

37 Fu, M. & Blackshear, P. J. RNA-binding proteins in immune regulation: a focus on CCCH zinc finger proteins. *Nat Rev Immunol* **17**, 130-143, doi:10.1038/nri.2016.129 (2017).

38 Takeuchi, O. Endonuclease Regnase-1/Monocyte chemotactic protein-1-induced protein-1 (MCPIP1) in controlling immune responses and beyond. *Wiley Interdiscip Rev RNA* **9**, doi:10.1002/wrna.1449 (2018).

39 Mino, T. *et al.* Regnase-1 and Roquin Regulate a Common Element in Inflammatory mRNAs by Spatiotemporally Distinct Mechanisms. *Cell* **161**, 1058-1073, doi:10.1016/j.cell.2015.04.029 (2015).

40 Adachi, A. *et al.* Production of acquired immunodeficiency syndrome-associated

retrovirus in human and nonhuman cells transfected with an infectious molecular clone. *J Virol* **59**, 284-291 (1986).

41 Salazar-Gonzalez, J. F. *et al.* Genetic identity, biological phenotype, and evolutionary pathways of transmitted/founder viruses in acute and early HIV-1 infection. *J Exp Med* **206**, 1273-1289, doi:10.1084/jem.20090378 (2009).

42 Salazar-Gonzalez, J. F. *et al.* Deciphering human immunodeficiency virus type 1 transmission and early envelope diversification by single-genome amplification and sequencing. *J Virol* **82**, 3952-3970, doi:10.1128/JVI.02660-07 (2008).

43 Van Heuverswyn, F. *et al.* Genetic diversity and phylogeographic clustering of SIVcpzPtt in wild chimpanzees in Cameroon. *Virology* **368**, 155-171, doi:10.1016/j.virol.2007.06.018 (2007).

44 Fenton-May, A. E. *et al.* Relative resistance of HIV-1 founder viruses to control by interferon-alpha. *Retrovirology* **10**, 146, doi:10.1186/1742-4690-10-146 (2013).

45 Parrish, N. F. *et al.* Phenotypic properties of transmitted founder HIV-1. *Proc Natl Acad Sci U S A* **110**, 6626-6633, doi:10.1073/pnas.1304288110 (2013).

46 Parrish, N. F. *et al.* Transmitted/Founder and Chronic Subtype C HIV-1 Use CD4 and CCR5 Receptors with Equal Efficiency and Are Not Inhibited by Blocking the Integrin alpha 4 beta 7. *Plos Pathogens* **8**, doi:ARTN e1002686 10.1371/journal.ppat.1002686 (2012).

47 Mashiba, M., Collins, D. R., Terry, V. H. & Collins, K. L. Vpr overcomes macrophage-specific restriction of HIV-1 Env expression and virion production. *Cell Host Microbe* **16**, 722-735, doi:10.1016/j.chom.2014.10.014 (2014).

48 McBride, M. S. & Panganiban, A. T. The human immunodeficiency virus type 1 encapsidation site is a multipartite RNA element composed of functional hairpin structures. *J Virol* **70**, 2963-2973 (1996).

49 Nakano, Y. *et al.* HIV-1 competition experiments in humanized mice show that APOBEC3H imposes selective pressure and promotes virus adaptation. *PLoS Pathog* **13**, e1006348, doi:10.1371/journal.ppat.1006348 (2017).

50 Gringhuis, S. I. *et al.* HIV-1 blocks the signaling adaptor MAVS to evade antiviral host defense after sensing of abortive HIV-1 RNA by the host helicase DDX3. *Nat Immunol* **18**, 225-235, doi:10.1038/ni.3647 (2017).

818 **Figure Legends**

819 **Fig. 1. Identification of N4BP1 as an antiretroviral restriction factor.**

820 **a**, HEK293T cells were co-transfected with pNL4-3 and one of 62 expression plasmids
821 (Supplementary Table 1) encoding putative RNA binding proteins. Forty-eight hours post
822 transfection, cell culture supernatants were harvested and used to infect TZM-bl reporter
823 cells to determine infectious virus yield. The data values of two technical replicates.
824 **b**, HEK293T cells were transfected with either pNL4-3 or pAD17 together with
825 increasing amounts of N4BP1 expression plasmid. Expression of HIV-1 Env and Gag,
826 and N4BP1 in cell lysates as well as Gag p24 in the culture supernatants was determined
827 by immunoblot analysis 48 hours post-transfection. β-Actin was used as the loading
828 control. The upper panel shows infectious virus yield relative to the empty vector control
829 determined by the TZM-bl reporter assay. n = 3 biological replicates. Individual points
830 and means ± s.d. are shown.
831 **c**, HEK293T cells were co-transfected with proviral clones of HIV-1 together with
832 increasing amounts of vector expressing N4BP1. 48 hours post-transfection, a TZM-bl
833 reporter assay was performed to measure the production of infectious virus in
834 supernatants. Infectious virus yield relative to the empty vector control is shown as mean
835 ± s.d of biological replicates (n = 3). TF, transmitted founder virus; CC chronic control
836 virus; 6-mo, virus isolated 6 months post infection.
837 *P* values were calculated using unpaired two-tailed Student's *t*-test. *P < 0.05; ***P <
838 0.005.
839
840 **Fig. 2. N4BP1 is upregulated upon IFN stimulation and restricts viral replication in**
841 **T cells.**
842 **a**, *N4BP1* mRNA levels were measured by RT-qPCR in Jurkat cells treated with IFN-α
843 from human leukocytes (1000 U/ml) for the indicated periods of time. Data are shown as
844 mean ± s.d. of biological replicates (n = 3).

b, Immunoblot analysis of N4BP1 in cell lysates from Jurkat cells treated with IFN-α for 48 hours. β-Actin was used as the loading control.

c, *N4BP*1 mRNA levels were measured by RT-qPCR in primary human $CD4^+$ T cells treated with IFN-α for 24 h. Individual points and means ± s.d. are shown (n = 3). *P < 0.05; ***P < 0.005.

d, Expression levels of *IFNB1*, *N4BP1*, *BST-2* and *ISG15* mRNAs were measured by qPCR in Jurkat cells infected with HIV-1 NL4-3 (MOI 0.01). Data are shown as mean ± s.d. of biological replicates (n = 3).

e, *N4BP1* mRNA levels in spleens from humanized mice 6 weeks after HIV-1 infection (n = 8) or mock treatment (n = 6).

f, Immunoblot analysis of N4BP1 in cell lysates from control and N4BP1-knockout Jurkat cells (left panel). N.S. Non-specific. Replication of HIV-1 NL4-3 (MOI 0.01) in N4BP1 knockout or control Jurkat cell lines (right panel). Infectivity of HIV-1 in the culture supernatants was measured by TZM-bl assay.

g, Immunoblot analysis of N4BP1 in cell lysates from control cells and N4BP1-knockout Jurkat cells inducibly reconstituted with N4BP1 by using the Tet-on system and doxycycline stimulation (Dox) for 24 hours (left panel). Replication of HIV-1 NL4-3 (MOI 0.01) in control or N4BP1 knockout Jurkat cell lines reconstituted with or without N4BP1 by Dox treatment (right panel). Infectivity of HIV-1 in the culture supernatants was measured by TZM-bl assay.

h, Immunoblot analysis of Jurkat cells stably expressing FLAG-tagged N4BP1 (left panel). Replication of HIV-1 NL4-3 (MOI 0.01 or 0.001) in FLAG-N4BP1 expressing or control Jurkat cell lines (right panel). Infectivity of HIV-1 in the culture supernatants was measured by TZM-bl assay.

P values were calculated using unpaired two-tailed Student's *t*-test. *P < 0.05; **P < 0.01; ***P < 0.005.

Fig. 3. N4BP1 is upregulated upon IFN stimulation and restricts HIV-1 infection in macrophages

a, Expression levels of *N4BP1* or *BST-2* mRNA were measured by RT-qPCR in macrophage-like THP-1 cells stimulated with IFN-α for the indicated periods of time. Data are shown as mean ± s.d. of biological replicates (n = 3).

b, Immunoblot analysis of N4BP1 and β-Actin in cell lysates from macrophage-like THP-1 cells stimulated with IFN-α for 48 hours.

c, Expression levels of *N4BP1* mRNA were measured by RT-qPCR in human primary MDMs stimulated with IFN-α for 24 hours. n = 3 biological replicates. Individual points and means ± s.d. are shown.

d, Expression levels of N4BP1 in human primary MDMs upon stimulation of IFN-α for 48 hours were determined by immunoblotting.

e, N4BP1 expression levels were normalized to β-Actin levels and the unstimulated sample was set to 100 %. n = 3 biological replicates. Individual points and means ± s.d. are shown.

f, Representative immunoblot analysis of human MDMs transfected with control siRNA or three different N4BP1-specific siRNAs (left panel). N4BP1 expression levels were normalized to β-Actin levels and the control siRNA sample was set to 100 %. Data are shown as mean values ± s.d. of 5 independent experiments.

g, Human MDMs treated with control or N4BP1-specific siRNA (#18638-#18640) were infected with HIV-1 AD8 and analyzed for infectious virus production 3 (n = 9) and 6 (n = 7) days post-infection (dpi). Shown are mean percentages ±s.d. relative to those detected in control cells (100%).

P values were calculated using unpaired two-tailed Student's *t*-test. *P < 0.05; **P < 0.01; ***P < 0.005.

Fig. 4. N4BP1 is a cellular RNase degrading HIV-1 RNA

a, The expression levels of viral mRNA were measured by RT-qPCR in HEK293T cells cotransfected with an N4BP1 expression plasmid or an empty vector control together with the indicated viral infectious clones. n = 3 biological replicates. Individual points and means ± s.d. are shown.

b, Domain architecture of human N4BP1.

c, A structural modeling of the RNase domain of N4BP1. Colors highlight the evolutionary conservation of amino acids. D623, D704, D705 and D723 forming the catalytic center of the RNase are indicated (Left panel). Amino acid sequence alignment of the partial RNase domain of N4BP1 orthologs from various species. "*"Fully conserved residue, ":"conservation between groups of strongly similar properties, "." conservation between groups of weakly similar properties (right panel).

d, Purified N4BP1, but not its D623N mutant, cleaves [^{32}P]-labeled RNA derived from a subgenomic sequence of HIV-1 NL4-3 *in vitro*.

e, Structural models of the RNase domains (residues 616-775) in WT and D623N human N4BP1.

f, Northern blot analysis of HIV viral RNAs in HEK293T cells co-transfected with pNL4-3 and vectors expressing N4BP1 or N4BP1 D623N. Ribosomal 28S and 18S RNAs were included as loading controls.

g, RNA-IP-qPCR assay in HEK293T cells transfected with pNL4-3 together with or without Flag-tagged N4BP1. Flag-tagged N4BP1 D623N was immunoprecipitated with anti-Flab Ab or control IgG 48 hours after transfection and co-precipitated RNAs were quantified by RT-qPCR. n = 3 biological replicates. Individual points and means ± s.d. are shown.

h, HEK293T cells were cotransfected with pNL4-3 and vectors expressing N4BP1 or N4BP1 D623N. Shown are the immunoblots of cellular extracts and viral particles in the culture supernatants.

i, Infectious virus yield of HIV-1 NL4-3 in HEK293T cells transfected with pNL4-3

926 together with expression plasmids for N4BP1 WT, N4BP1 D623N or an empty vector
927 control as assessed by TZM-bl reporter assay. Infectious virus yield relative to the empty
928 vector control is shown. n = 3 biological replicates. Individual points and means ± s.d. are
929 shown.
930 *P* values were calculated using unpaired two-tailed Student's *t*-test. *P < 0.05, **P <
931 0.001, ***P < 0.005.
932
933 **Fig. 5. TCR stimulation induces MALT1-mediated degradation of N4BP1**
934 **a**, Immunoblot analysis of N4BP1 levels in primary $CD4^+$ T cells treated with
935 IFN-γ (50 ng/ml), IL-2 (100 U/ml), PMA (50 ng/ml) plus ionomycin (500 nM) or
936 anti-CD3/CD28 antibody-coated beads for 24 hours.
937 **b**, N4BP1 protein levels in Jurkat cells stimulated with PMA plus ionomycin for the
938 indicated periods of time were determined by immunoblotting.
939 **c**, Immunoblot analysis of N4BP1 in parental or MALT1-deficient Jurkat cells stimulated
940 with PMA plus ionomycin for 1 hour.
941 **d**, N4BP1 protein levels in Jurkat cells stimulated with PMA plus ionomycin for 1 hour
942 with zVAD-fmk, a pan-caspase inhibitor (10 μM) or zVRPR-fmk, a MALT1 inhibitor
943 (100 μM).
944 **e**, Schematic representations of N4BP1 and its mutants. The epitope of the
945 N4BP1-specific antibody used in the present study is indicated.
946 **f**, The apparent molecular weight of N4BP1 and its truncation mutants was determined by
947 immunoblotting of transfected HEK293T cells.
948 **g**, Sequence-logo plot representing the amino acid frequencies at positions P4 to P3' in 16
949 previously identified MALT1 cleavage sites (Supplementary Fig. 10e).
950 **h**, Localization of the potential MALT1 cleavage site in N4BP1. Multiple sequence
951 alignment of different N4BP1 orthologs . "*"Fully conserved residue, "." conservation
952 between groups of weakly similar properties.

i, Cleavage of N4BP1 in HEK293T cells transfected with the indicated N-terminally Flag-tagged N4BP1 variants. Degradation of N4BP1 and emergence of the 72 kDa cleavage product were monitored by immunoblot with an anti-Flag antibody.

j, N4BP1 levels were determined by immunoblotting of Jurkat cells transfected with an empty vector or expression plasmids for Flag-N4BP1.

k, HEK293T cells were co-transfected with pNL4-3 and vectors expressing WT or mutant N4BP1. 48 hours post-transfection, a TZM-bl reporter assay was performed. Infectious virus yield relative to the empty vector control is shown. n = 3 biological replicates. Individual points and means ± s.d. are shown.

P values were calculated using unpaired two-tailed Student's *t*-test. ***P < 0.005.

Fig. 6. MALT1-mediated degradation of N4BP1 in latently HIV-1 infected cells contributes to viral reactivation.

a-b, Immunoblot analysis of N4BP1 and MALT1 in cell lysates from MALT1-deficient J-Lat10.6 (**a**), JNLGFP (**b**) or control cells stimulated with or without PMA (50 ng/ml) for 24 hours.

c-d, The expression levels of *tat/rev* and *gag* mRNA were quantified by qPCR in MALT1-deficient J-Lat10.6 (**c**) or JNLGFP cells (**d**) stimulated with PMA (50 ng/ml) for the indicated periods of time. Data are shown as mean ± s.d. of biological replicates (n = 3).

e-f, Immunoblot analysis of N4BP1 and Gag p24 proteins in cell lysates or culture supernatants from J-Lat10.6 (**e**) or JNLGFP cells (**f**), which inducibly express N4BP1 or N4BP1 R509A by the Tet-on system treating with Dox and were stimulated with PMA (10 ng/ml) for 24 hours. The levels of Gag p24 in the supernatants were quantified and indicated as the percentage of Dox (-) controls.

g, Immunoblot analysis of N4BP1 in control and N4BP1 KO JNLGFP cells generated by the CRISPR/Cas9 system. β-Actin was used as loading control.

h-**i**, N4BP1 KO JNLGFP cells were inducibly reconstituted with WT or R509A N4BP1 by the Tet-on system via Dox treatment, followed by stimulation with PMA (10 ng/ml) for 24 hours. Cell lysates and culture supernatants were collected and immunoblot analysis was performed to determine the expression of N4BP1, Gag and β-Actin proteins (**h**). The ratio of p24 expression in the culture supernatants between Dox (-) controls and Dox (+) WT or R509A N4BP1 expressing cells examined in (**h**) is shown in (**i**) (n = 3). Individual points and means ± s.d. are shown.

P values were calculated using unpaired two-tailed Student's *t*-test. *P < 0.05, **P < 0.001, ***P < 0.005.

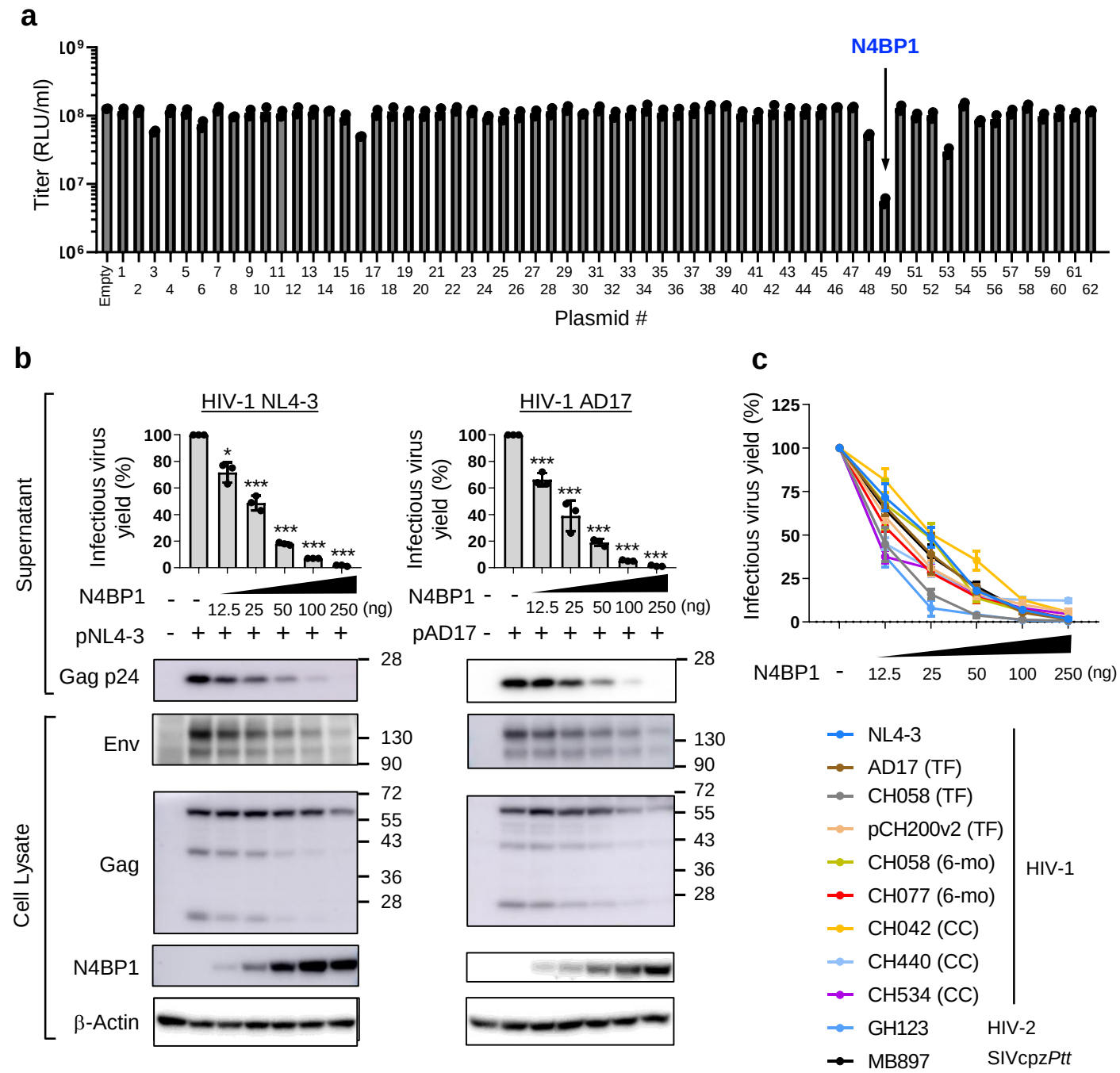
a
N4BP1
Titer (RLU/ml)
Plasmid #
b
HIV-1 NL4-3
HIV-1 AD17
Infectious virus yield (%)
N4BP1
pNL4-3
pAD17
12.5 25 50 100 250 (ng)
Supernatant
Cell Lysate
Gag p24
Env
Gag
N4BP1
β-Actin
c
Infectious virus yield (%)
NL4-3
AD17 (TF)
CH058 (TF)
pCH200v2 (TF)
CH058 (6-mo)
CH077 (6-mo)
CH042 (CC)
CH440 (CC)
CH534 (CC)
GH123
MB897
HIV-1
HIV-2
SIVcpzPtt

Figure 1

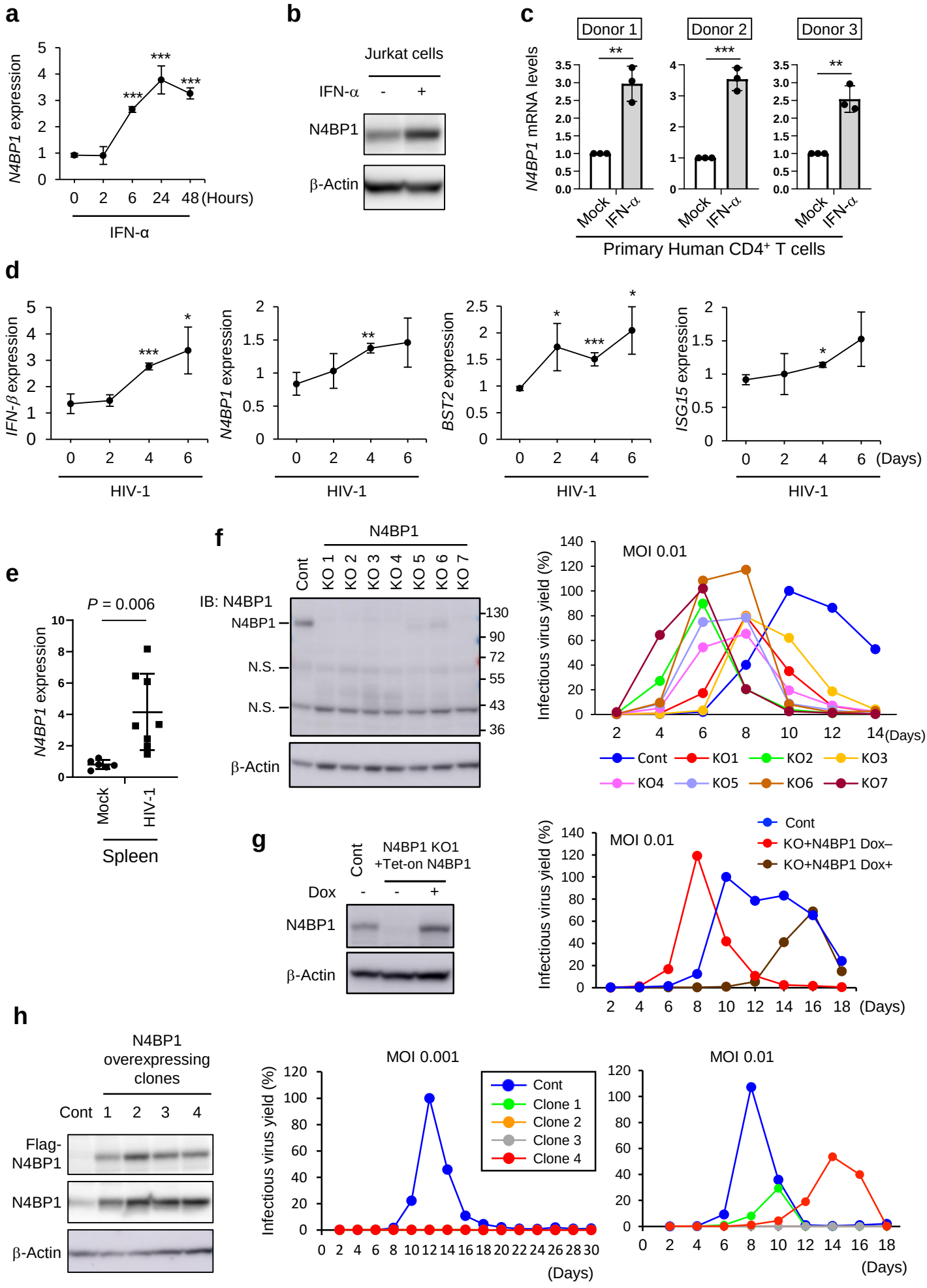
a
N4BP1 expression
0 2 6 24 48 (Hours)
IFN-α
b
Jurkat cells
IFN-α - +
N4BP1
β-Actin
c
Donor 1
Donor 2
Donor 3
N4BP1 mRNA levels
Mock
IFN-α
Primary Human CD4+ T cells
d
IFN-β expression
N4BP1 expression
BST2 expression
ISG15 expression
HIV-1
(Days)
e
P = 0.006
N4BP1 expression
Mock
HIV-1
Spleen
f
N4BP1
Cont KO 1 KO 2 KO 3 KO 4 KO 5 KO 6 KO 7
IB: N4BP1
N4BP1
N.S.
N.S.
β-Actin
130 90 72 55 43 36
MOI 0.01
Infectious virus yield (%)
(Days)
Cont KO1 KO2 KO3 KO4 KO5 KO6 KO7
g
Cont
N4BP1 KO1 +Tet-on N4BP1
Dox - - +
N4BP1
β-Actin
MOI 0.01
Cont
KO+N4BP1 Dox–
KO+N4BP1 Dox+
h
N4BP1 overexpressing clones
Cont 1 2 3 4
Flag-N4BP1
N4BP1
β-Actin
MOI 0.001
MOI 0.01
Cont
Clone 1
Clone 2
Clone 3
Clone 4

Figure2

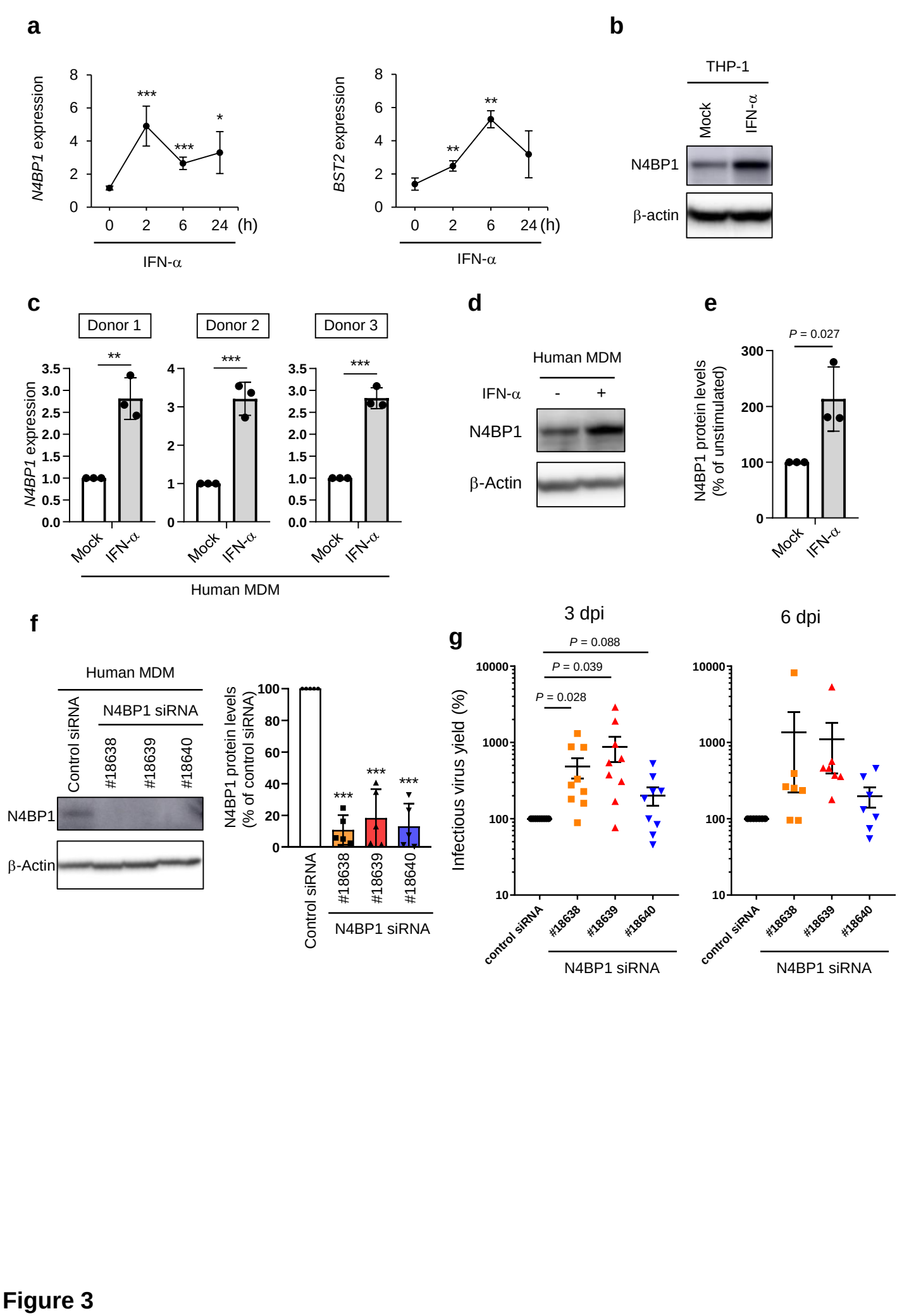
a
N4BP1 expression
BST2 expression
IFN-α
0 2 6 24 (h)
b
THP-1
Mock
IFN-α
N4BP1
β-actin
c
Donor 1
Donor 2
Donor 3
N4BP1 expression
Mock
IFN-α
Human MDM
d
Human MDM
IFN-α
N4BP1
β-Actin
e
P = 0.027
N4BP1 protein levels (% of unstimulated)
f
Human MDM
Control siRNA
N4BP1 siRNA
#18638
#18639
#18640
N4BP1
β-Actin
N4BP1 protein levels (% of control siRNA)
g
3 dpi
6 dpi
P = 0.088
P = 0.039
P = 0.028
Infectious virus yield (%)
control siRNA
N4BP1 siRNA

Figure 3

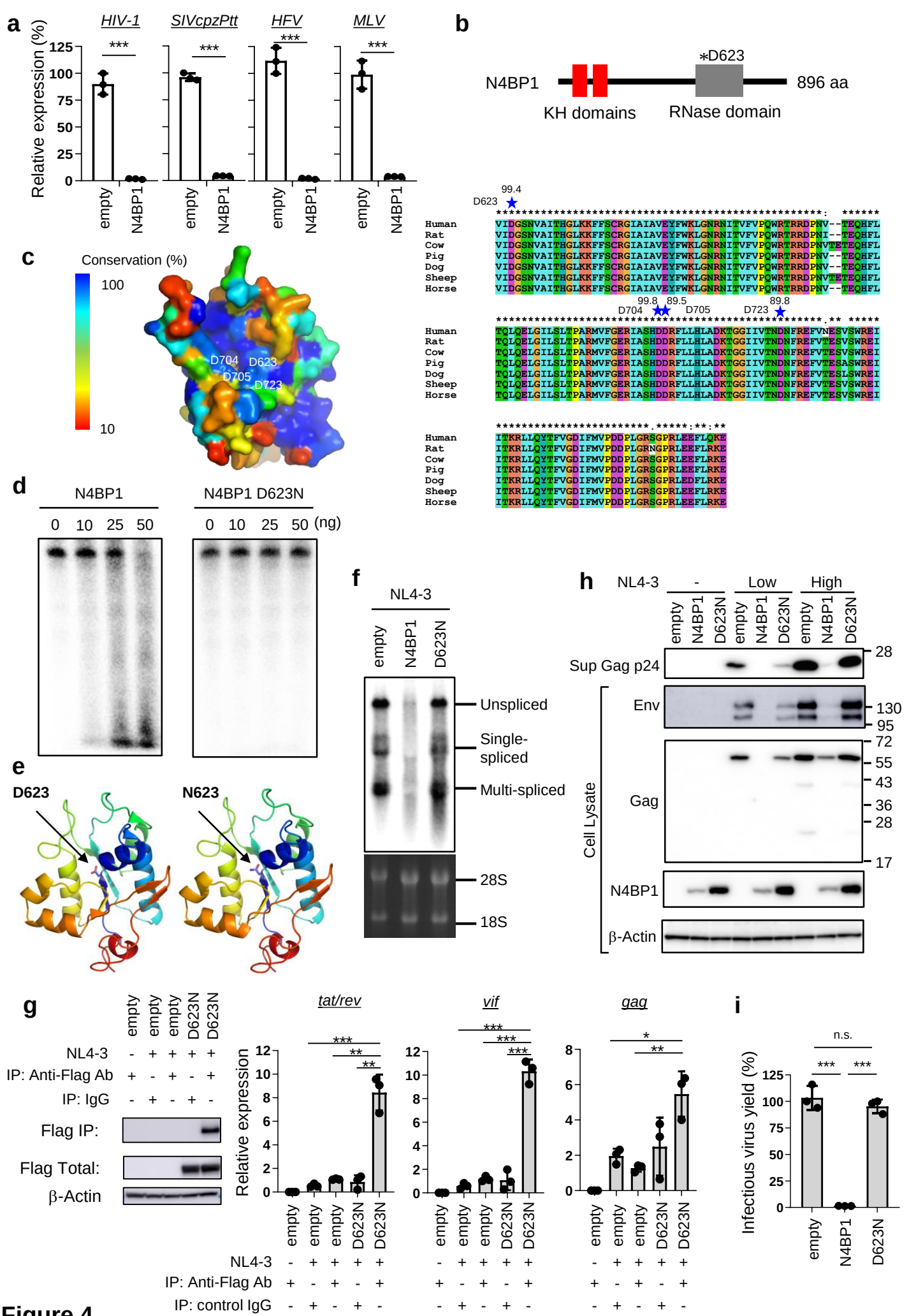
a
HIV-1
SIVcpzPtt
HFV
MLV
Relative expression (%)
empty
N4BP1
b
N4BP1
*D623
896 aa
KH domains
RNase domain
D623
99.4
D704
99.8
89.5
D705
89.8
D723
Human
Rat
Cow
Pig
Dog
Sheep
Horse
c
Conservation (%)
100
10
D704
D623
D705
D723
d
N4BP1
N4BP1 D623N
0 10 25 50 (ng)
e
D623
N623
f
NL4-3
empty
N4BP1
D623N
Unspliced
Single-spliced
Multi-spliced
28S
18S
h
NL4-3
-
Low
High
Sup Gag p24
Env
Gag
N4BP1
β-Actin
Cell Lysate
28
130
95
72
55
43
36
28
17
g
NL4-3
IP: Anti-Flag Ab
IP: IgG
Flag IP:
Flag Total:
β-Actin
tat/rev
vif
gag
Relative expression
IP: control IgG
i
Infectious virus yield (%)
n.s.

Figure 4

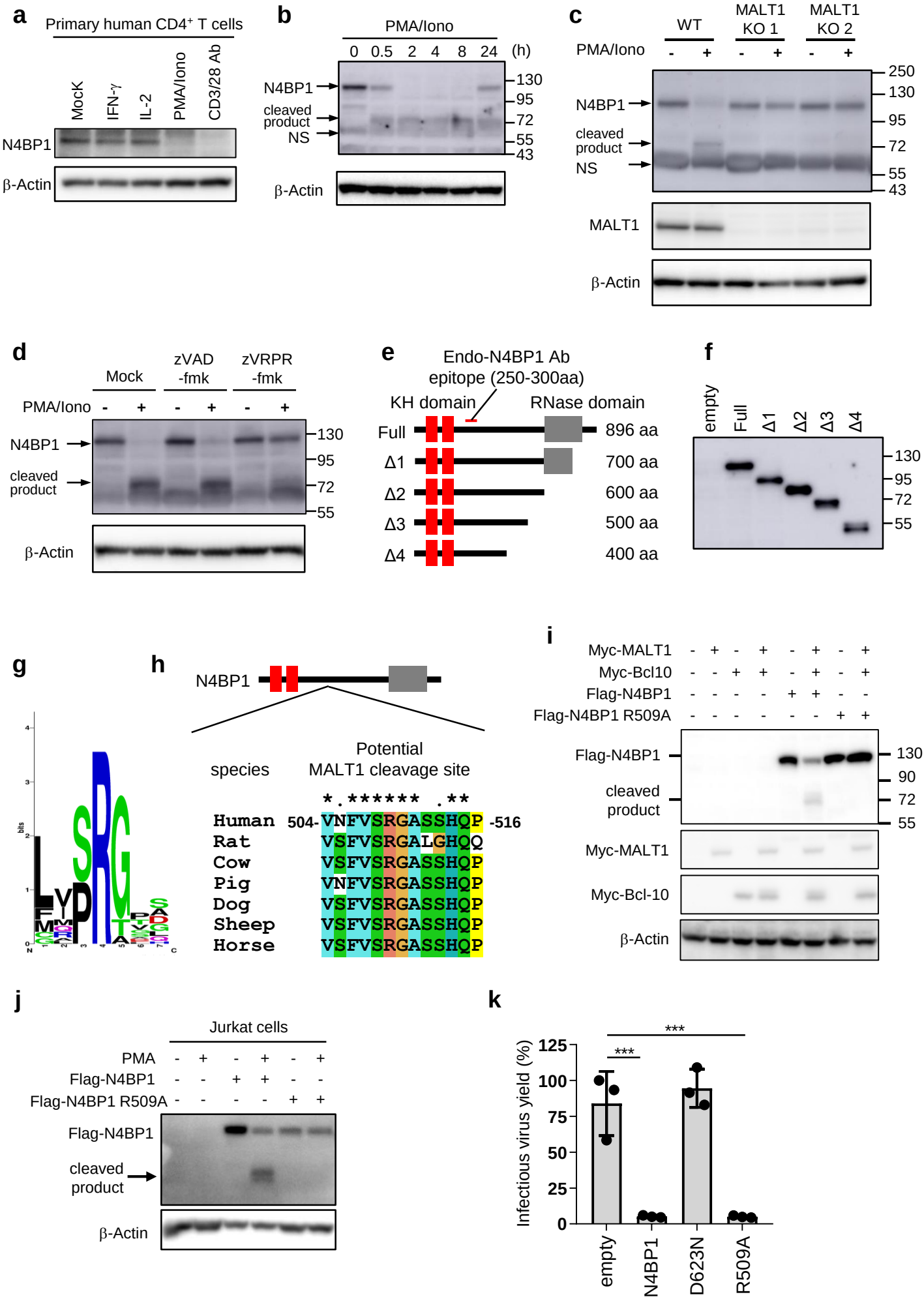
a
Primary human CD4+ T cells
MockK
IFN-γ
IL-2
PMA/Iono
CD3/28 Ab
N4BP1
β-Actin
b
PMA/Iono
0 0.5 2 4 8 24 (h)
N4BP1
cleaved product
NS
130
95
72
55
43
β-Actin
c
WT
MALT1 KO 1
MALT1 KO 2
PMA/Iono - + - + - +
N4BP1
cleaved product
NS
250
130
95
72
55
43
MALT1
β-Actin
d
Mock
zVAD -fmk
zVRPR -fmk
PMA/Iono - + - + - +
N4BP1
cleaved product
130
95
72
55
β-Actin
e
Endo-N4BP1 Ab epitope (250-300aa)
KH domain
RNase domain
Full 896 aa
Δ1 700 aa
Δ2 600 aa
Δ3 500 aa
Δ4 400 aa
f
empty
Full
Δ1
Δ2
Δ3
Δ4
130
95
72
55
g
bits
h
N4BP1
species
Potential MALT1 cleavage site
Human 504-VNFVSRGASSHQP-516
Rat VSFVSRGALGHQQ
Cow VSFVSRGASSHQP
Pig VNFVSRGASSHQP
Dog VSFVSRGASSHQP
Sheep VSFVSRGASSHQP
Horse VSFVSRGASSHQP
i
Myc-MALT1 - + - + - + - +
Myc-Bcl10 - - + + - + - +
Flag-N4BP1 - - - - + + - -
Flag-N4BP1 R509A - - - - - - + +
Flag-N4BP1
cleaved product
130
90
72
55
Myc-MALT1
Myc-Bcl-10
β-Actin
j
Jurkat cells
PMA - + - + - +
Flag-N4BP1 - - + + - -
Flag-N4BP1 R509A - - - - + +
Flag-N4BP1
cleaved product
β-Actin
k
Infectious virus yield (%)
125
100
75
50
25
0
***
***
empty
N4BP1
D623N
R509A

Figure 5

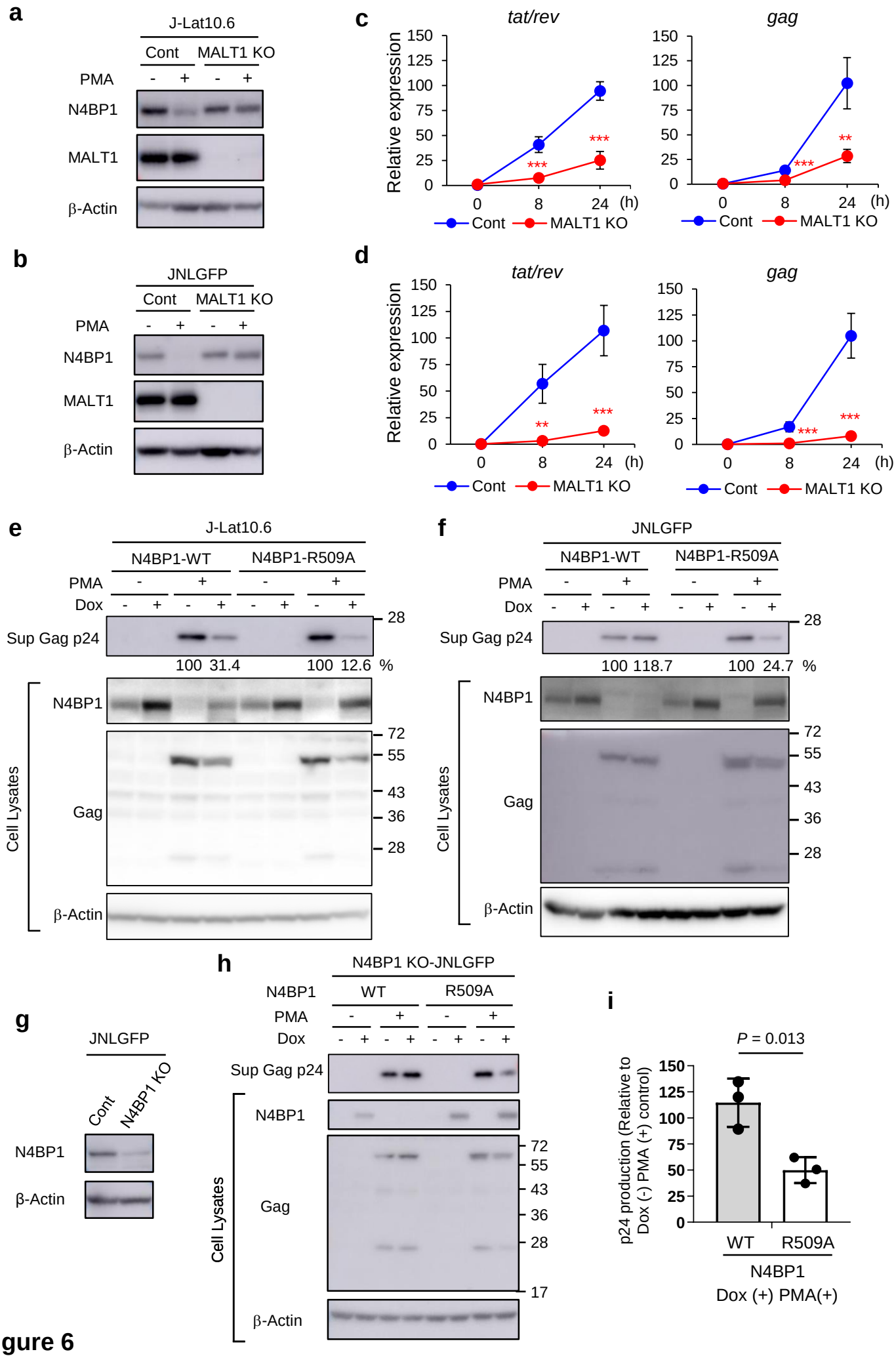
a
J-Lat10.6
Cont
MALT1 KO
PMA
N4BP1
MALT1
β-Actin
b
JNLGFP
c
tat/rev
gag
Relative expression
Cont
MALT1 KO
d
e
J-Lat10.6
N4BP1-WT
N4BP1-R509A
Dox
Sup Gag p24
100 31.4
100 12.6
%
Cell Lysates
Gag
f
JNLGFP
100 118.7
100 24.7
g
N4BP1 KO
h
N4BP1 KO-JNLGFP
WT
R509A
i
P = 0.013
p24 production (Relative to Dox (-) PMA (+) control)
Dox (+) PMA(+)

Figure 6

Supplemental Information for

N4BP1 restricts HIV-1 and its inactivation by MALT1 promotes viral reactivation

Daichi Yamasoba[1,2,5], Kei Sato[3,6,7], Takuya Ichinose[1,2,5], Tomoko Imamura[2], Lennart Koepke[8], Simone Joas[8], Elisabeth Reith[8], Dominik Hotter[8], Naoko Misawa[3], Kotaro Akaki[1,2], Takuya Uehata[1,2], Takashi Mino[1,2], Sho Miyamoto[4], Takeshi Noda[4], Akio Yamashita[9], Daron M. Standley[10], Frank Kirchhoff[8], Daniel Sauter[8], Yoshio Koyanagi[3] and Osamu Takeuchi[1,2*]

[1]Department of Medical Chemistry, Graduate School of Medicine, [2]Laboratory of Infection and Prevention, [3]Laboratory of Systems Virology, [4]Laboratory of Ultrastructural Virology, Institute for Frontier Life and Medical Sciences, [5]Graduate School of Biostudies, Kyoto University, 53 Shogoin Kawahara-cho, Sakyo-ku, Kyoto 606-8507, Japan
[6]CREST, Japan Science and Technology Agency, Saitama 322-0012, Japan.
[7]Department of Systems Virology, Institute for Medical Science, the University of Tokyo, 4-6- 1 Shirokanedai, Minato-ku, Tokyo 108-8639, Japan
[8]Institute of Molecular Virology, Ulm University Medical Center, 89081 Ulm, Germany
[9]Department of Molecular Biology, Yokohama City University School of Medicine, Kanagawa 236-0004, Japan
[10]Department of Genome Informatics, Genome Information Research Center, Research Institute for Microbial Diseases, Osaka University, 3 Yamada-oka, Suita, Osaka 565-0871, Japan
*e-mail: otake@mfour.med.kyoto-u.ac.jp.

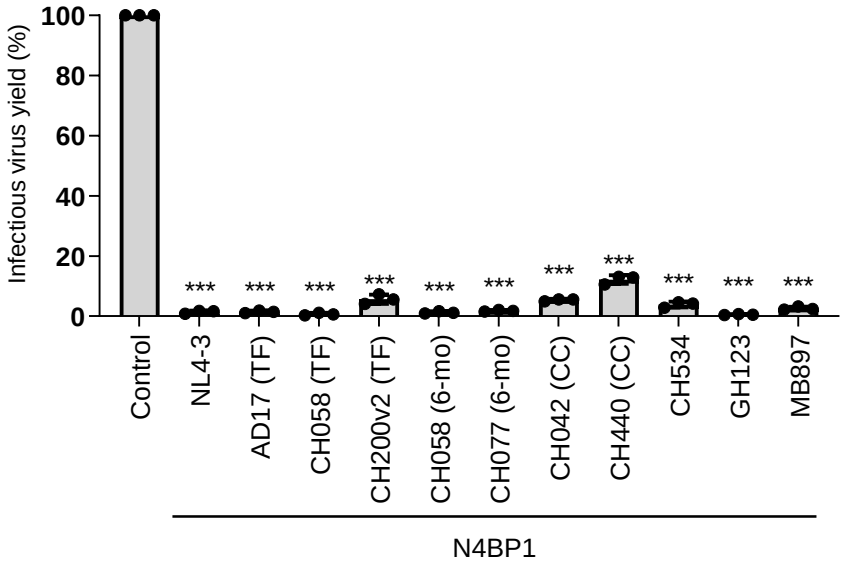

Supplementary Figure 1. N4BP1 inhibits various clones of HIV-1, HIV-2 and SIVcpz*Ptt*.

HEK293T cells were transfected with proviral clones expressing NL4-3, AD17 (TF), CH058 (TF), CH200v2 (TF), CH058 (6-mo), CH077 (6-mo), CH042 (CC), CH534 (CC), CH440 (CC), GH123 (HIV-2) or MB897 (SIVcpz*Ptt*) (250 ng each), together with the N4BP1 expression plasmid (250 ng). Forty eight hours post-transfection, a TZM-bl reporter assay was performed to measure the production of infectious virus in the cell culture supernatants. Infectious virus yields normalized to the empty vector control are shown as mean values ± s.d. of biological replicates (n = 3). *P* values were calculated using unpaired two-tailed Student's *t*-test. ***P < 0.005.

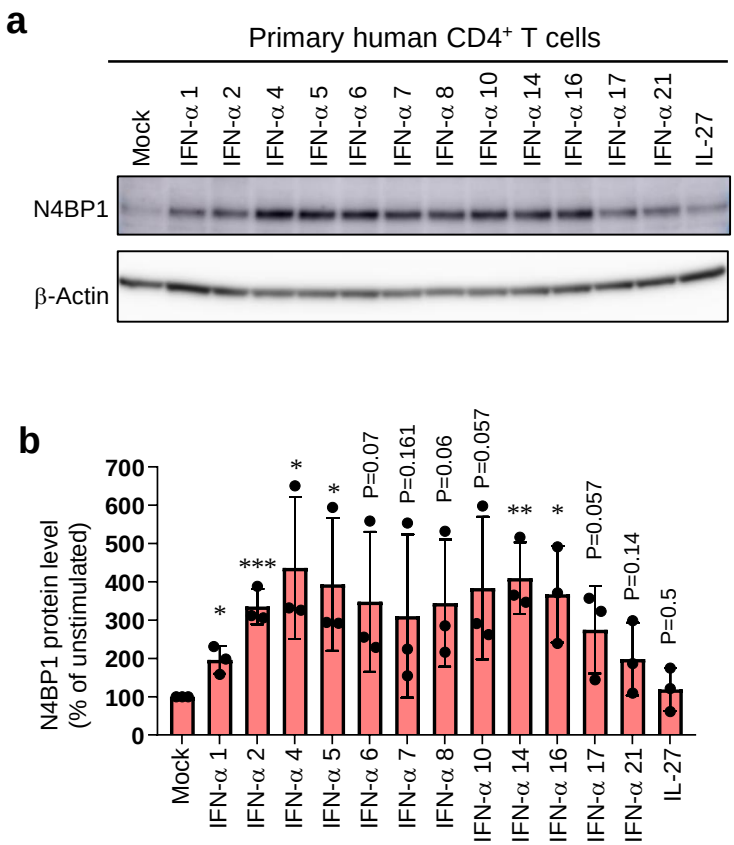

Supplementary Figure 2. N4BP1 expression is induced by various IFN-α subtypes in human primary CD4⁺ T cells.

(**a**) Immunoblot analysis for the expression of N4BP1 in human primary CD4⁺ T cells stimulated with indicated IFN-α subtypes (50 ng/ml each) or IL-27 (5 ng/ml) for 3 days. β-Actin was used as loading controls. Data are representative of three independent experiments.

(**b**) N4BP1 expression levels were determined by immunoblotting as shown in (a) and normalized to β-actin levels. The unstimulated sample was set to 100%. Data shown are mean values ± s.d. of immunoblot data derived from 3 individual donors. *P* values were calculated using unpaired two-tailed Student's *t*-test. *P < 0.05; **P < 0.01; ***P < 0.005.

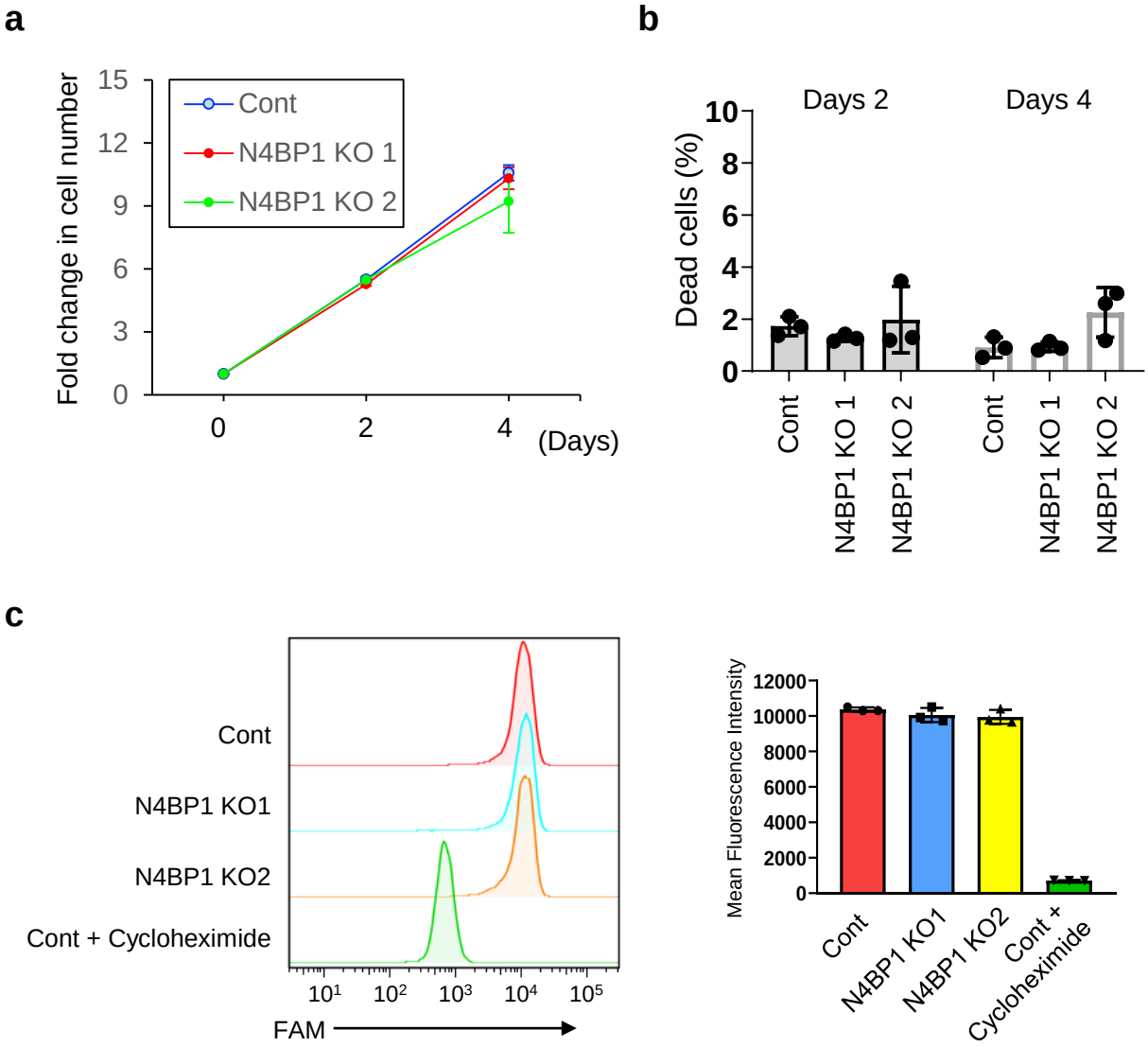

Supplementary Figure 3. N4BP1 deficiency in Jurkat cells does not affect growth, cell death or global protein synthesis

(**a**) N4BP1 KO Jurkat cells (clones 1 and 2) and control (Cont) cells were cultivated for 2 and 4 days and changes in cell numbers are shown. Data are shown as mean ± s.d. of biological replicates (n = 3).
(**b**) Cells in a were analyzed by Flow cytometry (FACSVerse; BD) after propidium iodide staining. Individual points and means ± s.d. are shown (n = 3).
(**c**) Control and N4BP1 KO Jurkat cells were cultured for 1 day. As negative control, some control cells were treated with a protein synthesis inhibitor, Cycloheximide (Cayman Chemical) for 30 min. Then the cells were harvested, and translating polypeptides were labeled with O-Propargyl-Puromycin (OPP) for 30 min at 37 ˚ C followed by staining with 5 FAM Azide using the Protein Synthesis Assay kit (Cayman Chemical). The cells were analyzed by Flow cytometry (FACSVerse; BD). Representative histograms for the levels of translating polypeptides (FAM) are shown (Left panel). Mean Fluorescence Intensities from the experiments were shown in the right panel. n = 3 biologically independent samples. Individual points and means ± s.d. are shown.

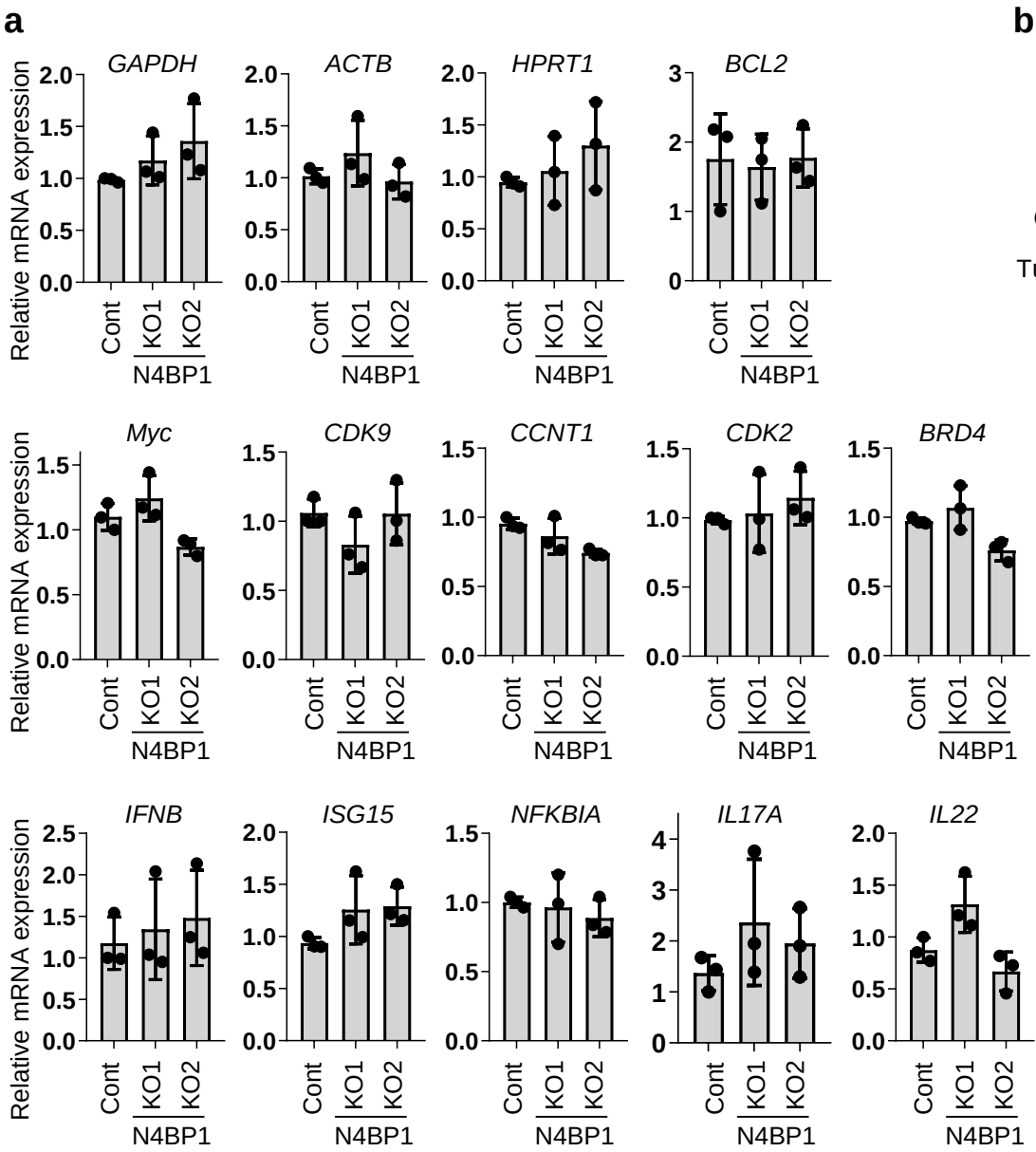

Supplementary Figure 4. N4BP1 deficiency does not affect the expression of a set of house keeping genes, genes involved in cell cycling, apoptosis, IFN responses, IL17A and IL22 in N4BP1 KO Jurkat cells.

(**a**) Total RNA was prepared from control and N4BP1 KO Jurkat cells cultured for 1 day, and expression levels of the indicated genes including house-keeping genes (*GAPDH*, *ACTB* or *HPRT*), the anti-apoptotic gene *BCL2*, cell cycle-related genes (*MYC*, *CDK9*, *CCNT1*, *CDK2* and *BRD4*), *IFNB* and inflammatory and anti-inflammatory genes (*NFKBIA*, *IL17A* and *IL22*) were determined by RT-qPCR. Individual points and means ± s.d. are shown. Data are from n = 3 biologically independent samples.
(**b**) Cell lysates were prepared from control and N4BP1 KO Jurkat cells cultured for 1 day, and the expression of N4BP1, GAPDH, Tubulin-α and IκBα proteins was determined by immunoblot analysis. β-actin was used as loading controls. Data are representative of two independent experiments

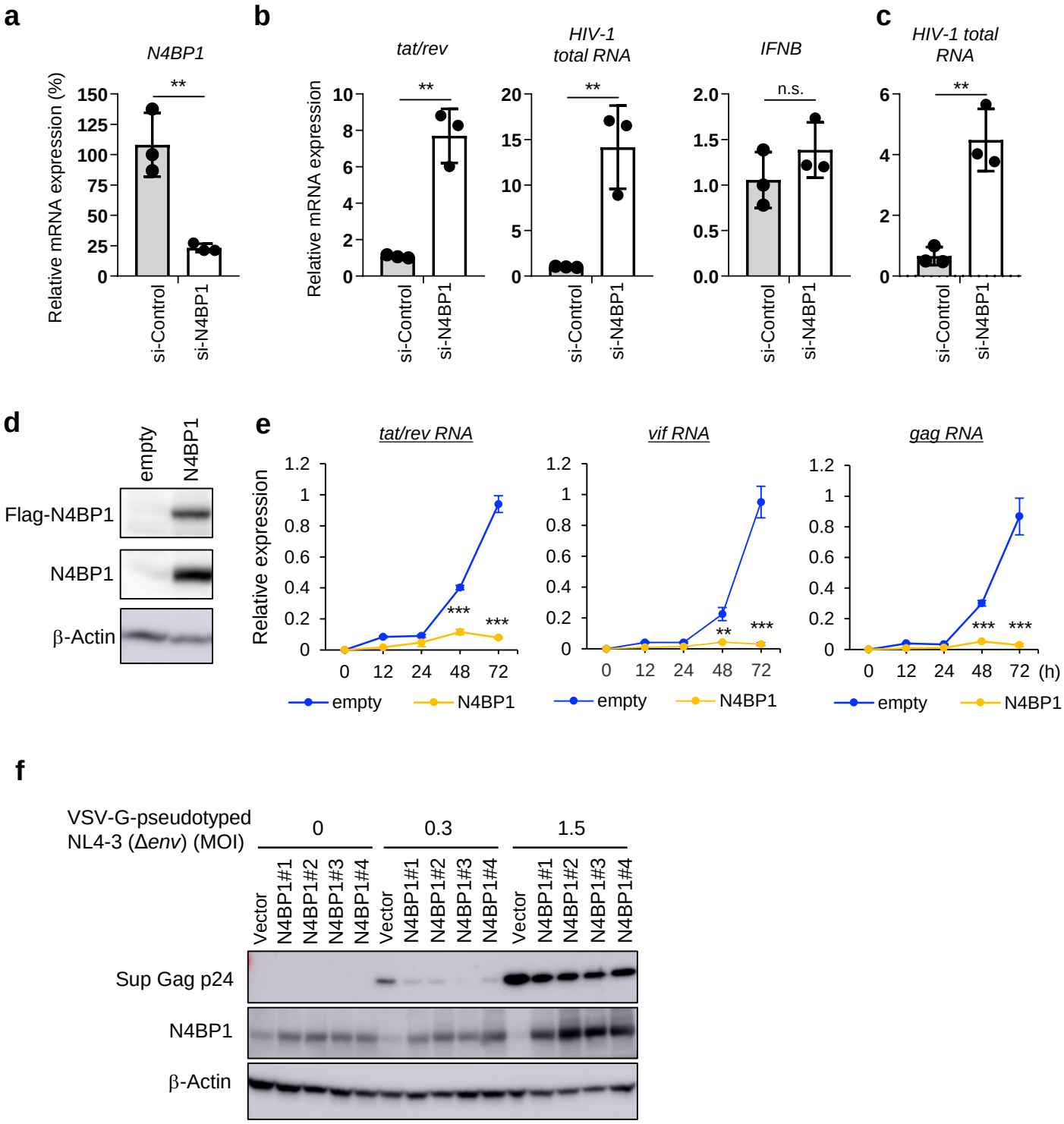
a
N4BP1
Relative mRNA expression (%)
150
125
100
75
50
25
0
**
si-Control
si-N4BP1
b
tat/rev
HIV-1 total RNA
IFNB
Relative mRNA expression
10
8
6
4
2
0
20
15
10
5
2.0
1.5
1.0
0.5
0.0
**
n.s.
c
HIV-1 total RNA
6
4
2
d
empty
N4BP1
Flag-N4BP1
N4BP1
β-Actin
e
tat/rev RNA
vif RNA
gag RNA
Relative expression
1.2
1
0.8
0.6
0.4
0.2
0
0 12 24 48 72 (h)
***
empty
N4BP1
f
VSV-G-pseudotyped NL4-3 (Δenv) (MOI)
0
0.3
1.5
Vector
N4BP1#1
N4BP1#2
N4BP1#3
N4BP1#4
Sup Gag p24
N4BP1
β-Actin

Supplementary Figure 5. N4BP1 restricts HIV-1 in Jurkat cells.

(**a**) N4BP1 expression levels were determined by RT-qPCR in Jurkat cells transfected with N4BP1 specific siRNA for 72 hours. n = 3 biological replicates. Individual points and means ± s.d. are shown.

(**b** and **c**) siRNA-treated Jurkat cells were infected with HIV-1 NL4-3. Seventy two hours post-infection, *IFNB* and viral mRNA expression levels in the cell lysates (**b**) and the culture supernatants (**c**) were determined by qPCR. n = 3 biological replicates. Individual points and means ± s.d. are shown.

(**d**) Immunoblot analysis for Flag-tagged N4BP1, endogenous N4BP1 and β-Actin in cell lysates from Jurkat cells stably expressing N4BP1.

(**e**) Expression levels of *tat/rev*, *vif* or *gag* RNA were measured by qPCR in Jurkat cells stably expressing N4BP1 or the respective parental cell line following infection with HIV-1 for the indicated periods. Data are shown as mean values ± s.d. of technical replicates (n = 3).

(**f**) N4BP1-stably expressing Jurkat cells and control cells were infected with VSV-G-pseudotyped HIV-1 NL4-3 Δenv. Forty eight hours post infection, culture supernatants (Sup) and cell lysates were collected and analyzed by immunoblotting for the expression of Gag p24 in the culture supernatants (Sup), and N4BP1 and β-Actin in cell lysates.

P values were calculated using unpaired two-tailed Student's *t*-test. *P < 0.05; **P < 0.01; ***P < 0.005. n.s. not significant. Data are representative three (a-e) and two (f) independent experiments.

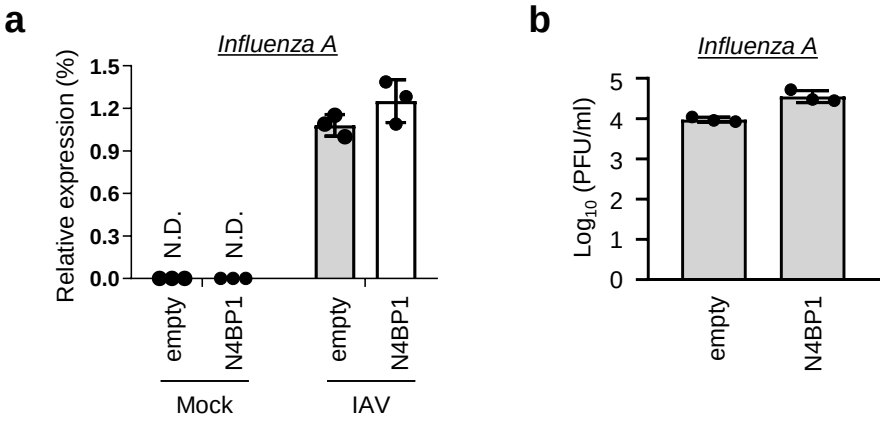

Supplementary Figure 6. N4BP1 does not suppress influenza virus.

(**a**) HEK293T cells stably expressing N4BP1 or control cells were infected with Influenza A virus (PR8 strain) for 24 hours before the expression level of viral mRNA for segment 4 (HA) was measured by qPCR. N.D., Not detected. n = 3 biological replicates. Individual points and means ± s.d. are shown.

(**b**) HEK293T cells stably expressing N4BP1 or control cells were infected with Influenza A virus (WSN strain) at an MOI of 1 X 10^{-3}, and the culture media were harvested 24 hours postinfection. The virus titers were determined by using plaque assays on MDCK cells. Individual points and means ± s.d. are shown. Data are from n = 3 biologically independent samples.

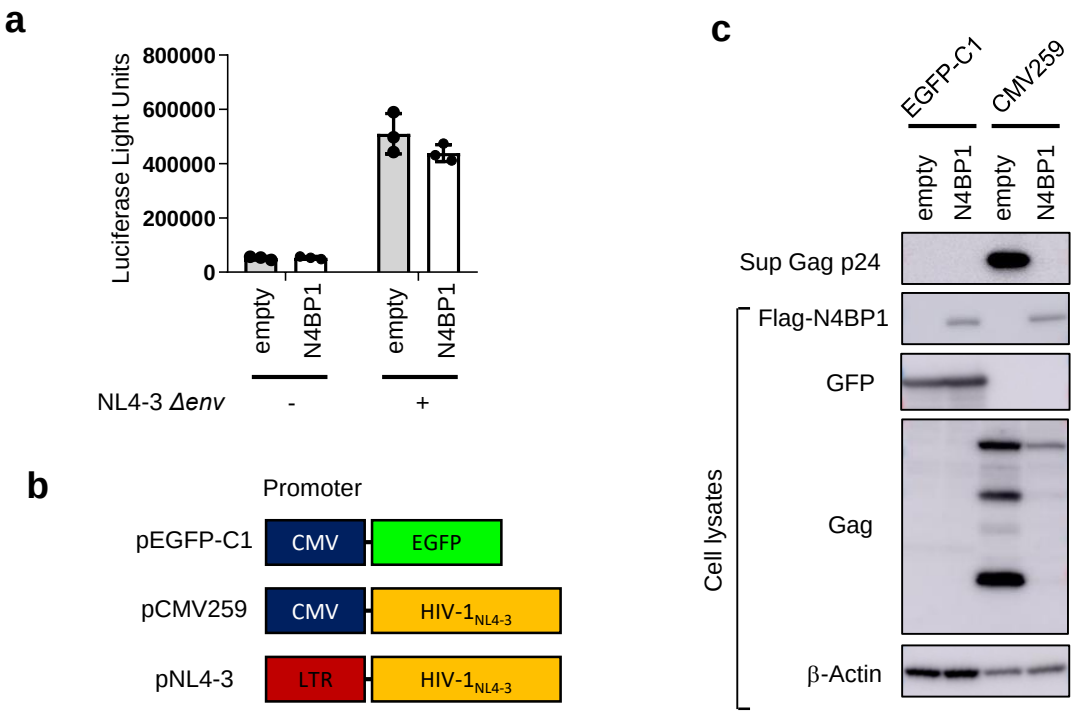

Supplementary Figure 7. N4BP1 inhibits HIV-1 at the post-transcriptional level.

(**a**) LTR promotor activity was determined in TZM-bl cells cotransfected with N4BP1 and HIV-1 NL4-3 Δ*env* expressing plasmids. n = 3 biological replicates. Individual points and means ± s.d. are shown.
(**b**) Schematic representation of plasmids used in (**c**). The pEGFPC1 plasmid (Clontech) expresses EGPF protein under the control of CMV promoter. pCMV259 expresses HIV-1 NL4-3 under the CMV promoter instead of LTR (pNL4-3).
(**c**) HEK293T cells were transfected with pEGFP-C1 or pCMV259 together with or without Flag-N4BP1 plasmids. Expression of Gag p24 in the culture supernatants (Sup) as well as the expression of Flag-N4BP1, GFP, Gag and β-Actin in the cell lysates were determined by immunoblotting 48 hours after transfection. Data are representative of two independent experiments.

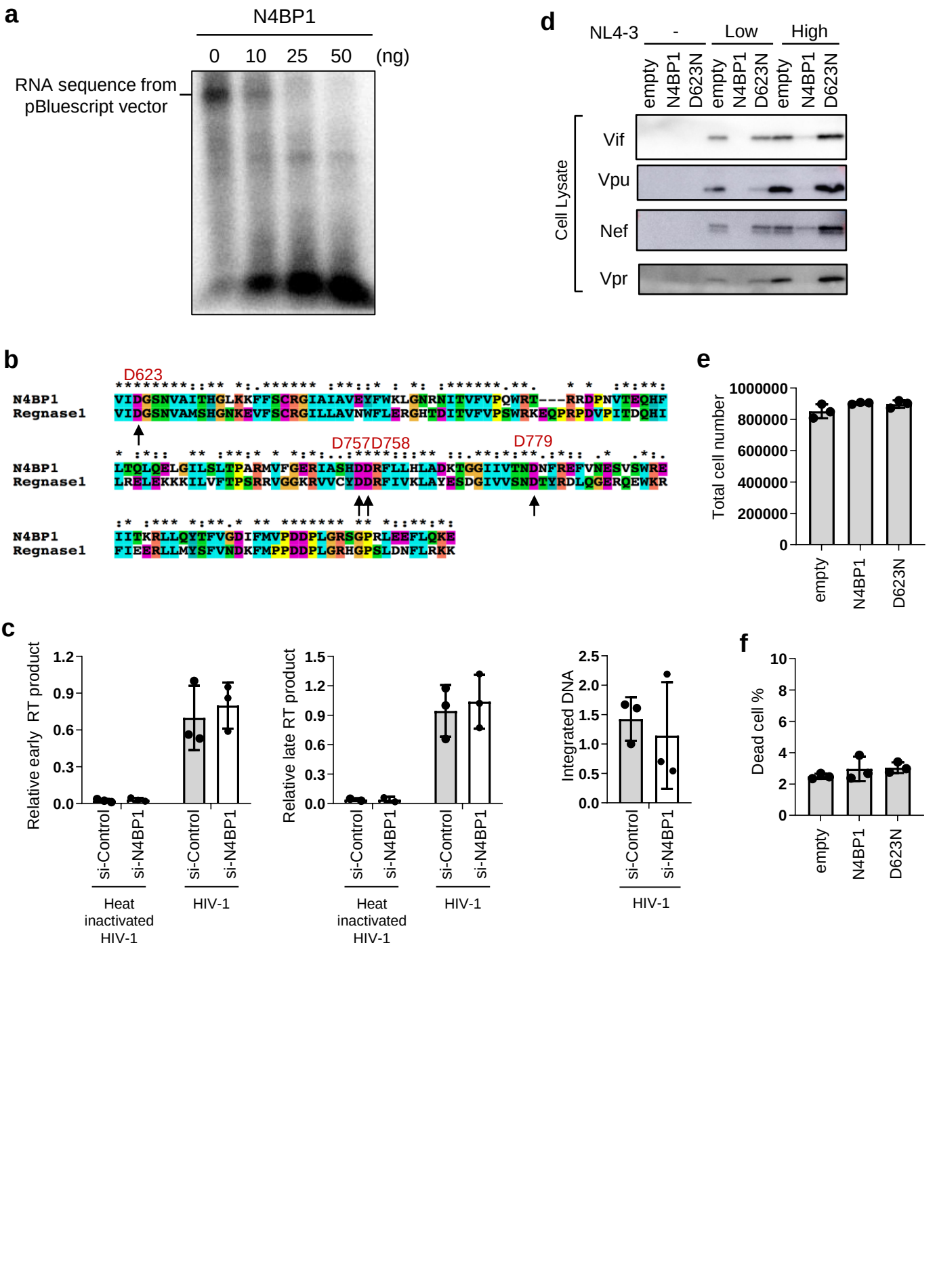
a
N4BP1
0 10 25 50 (ng)
RNA sequence from pBluescript vector
d
NL4-3 - Low High
empty N4BP1 D623N empty N4BP1 D623N empty N4BP1 D623N
Cell Lysate
Vif
Vpu
Nef
Vpr
b
D623
D757D758
D779
N4BP1 VIDGSNVAITHGLKKFFSCRGIAIAVEYFWKLGNRNITVFVPQWRT---RRDPNVTEQHF
Regnase1 VIDGSNVAMSHGNKEVFSCRGILLAVNWFLERGHTDITVFVPSWRKEQPRPDVPIIDQHI
N4BP1 LTQLQELGILSLTPARMVFGERIASHDDRFLLHLADKTGGIIVTNDNFREFVNESVSWRE
Regnase1 LRELEKKKILVFTPSRRVGGKRVVCYDDRFIVKLAYESDGIVVSNDTYRDLQGERQEWKR
N4BP1 IITKRLLQYTFVGDIFMVPDDPLGRSGPRLEEFLQKE
Regnase1 FIEERLLMYSFVNDKFMPPDDPLGRHGPSLDNFLRKK
e
Total cell number
1000000
800000
600000
400000
200000
0
empty N4BP1 D623N
c
Relative early RT product
1.2 0.9 0.6 0.3 0.0
si-Control si-N4BP1 si-Control si-N4BP1
Heat inactivated HIV-1
HIV-1
Relative late RT product
1.5 1.2 0.9 0.6 0.3 0.0
si-Control si-N4BP1 si-Control si-N4BP1
Heat inactivated HIV-1
HIV-1
Integrated DNA
2.5 2.0 1.5 1.0 0.5 0.0
si-Control si-N4BP1
HIV-1
f
Dead cell %
10 8 6 4 2 0
empty N4BP1 D623N

Supplementary Figure 8. N4BP1 inhibits HIV-1 at the late stage depending on its RNase activity.

(**a**) Purified N4BP1 was subjected to the *in vitro* cleavage assay using [^{32}P]-labeled RNA derived from a part of the pBluescript vector.

(**b**) Multiple sequence alignment of the N4BP1 and Regnase-1 RNase domains. Arrows indicate conserved Asp residues in the catalytic domain.

(**c**) N4BP1 knockdown Jurkat cells exposed to HIV-1 NL4-3 (MOI; 0.1) or heat-inactivated HIV-1 NL4-3 at 37° C for 2 hours. Total DNA was isolated 12 hours after treatment, and amounts of early RT (R/U5) and late RT (U5/gag) products and integrated provirus were quantified by qPCR in. n = 3 biological replicates. Individual points and means ± s.d. are shown.

(**d**) HEK293T cells were cotransfected with pNL4-3 and vectors expressing N4BP1 or N4BP1 D623N. Shown are the immunoblots for the expression of Vif, Vpu, Nef and Vpr in cell lysates prepared 48 hours after transfection.

(**e** and **f**) HEK293T cells were transfected with WT or D623N N4BP1 plasmids and cells were counted (**e**) or analyzed by flow cytometry after propidium iodide staining (**f**) 48 h later. Data are mean ± s.d. of biological replicates. Data are representative three (c and d) and two (a) independent experiments.

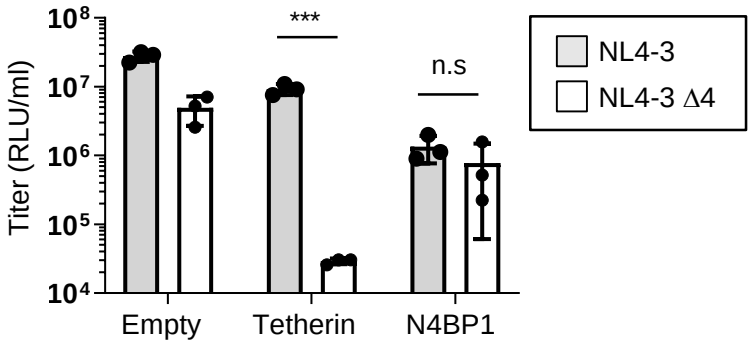

Supplementary Figure 9. N4BP1 is not antagonized by accessory proteins of HIV-1 NL4-3.

HEK293T cells were transfected with an expression plasmid for N4BP1, Tetherin or empty vector together with NL4-3 wild type or NL4-3 Δ4. The latter does not express any of the accessory proteins encoded by HIV-1 (i.e. Vpu, Vif, Vpr and Nef). Infectious virus production was measured by TZM-bl assay 48 hours after transfection = 3 biological replicates. Individual points and means ± s.d. are shown. *P* values were calculated using unpaired two-tailed Student's *t*-test. ***P < 0.005. n.s. not significant.

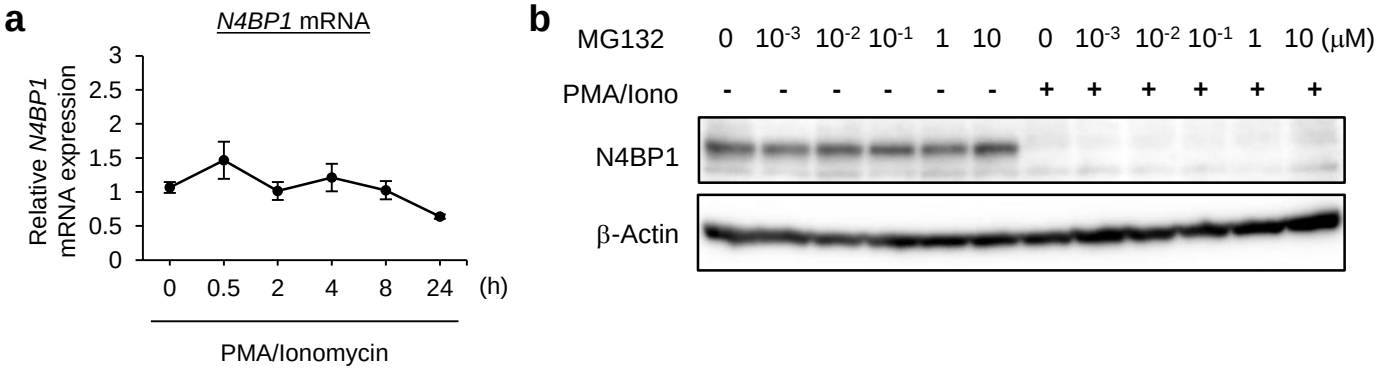

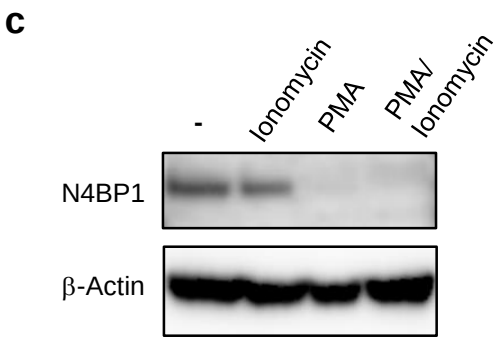

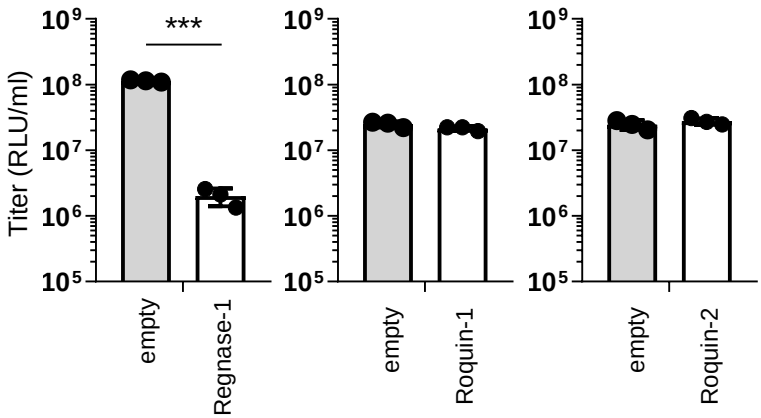

e

Protein	Previously reported MALT1 cleavage sites
mRoquin-2	LIPRGTD
hRoquin-2	LISRTDS
mRoquin-1	LIPRGTD… MVPRGSQ
hRoquin-1	LIPRGTD… MVPRGSQ
mRegnase-1	LVPRGGS
hRegnase-1	LVPRGGG
hA20	GASRGEA
mBcl-10	LRSRALS
hBcl-10	LRSRTVS
mRelB	LVSRGPA
hRelB	LVSRGPA
hNIK	CLSRGAH
mCYLD	FMSRGVG
hCYLD	FMSRGVG
hHOIL1	LQPRGPL
mHOIL1	LQSRGPL

Supplementary Figure 10. N4BP1 is degraded by MALT1 and contribution of other MALT1 substrates in the inhibition of HIV-1.

(**a**) Expression levels of *N4BP1* mRNA were determined by RT-qPCR in Jurkat cells stimulated with PMA (50 ng/ml) plus ionomycin (1 μM) for the indicated periods of time. Data are shown as mean ± s.d. of biological replicates (n = 3).

(**b**) N4BP1 expression levels were determined by immunoblotting in cell lysates from Jurkat cells stimulated with PMA plus ionomycin for 1 hour with or without the indicated concentrations of proteasome inhibitor MG132. β-Actin was used as loading controls. Data are representative of three independent experiments.

(**c**) Immunoblot analysis of N4BP1 in cell lysates from Jurkat cells stimulated with PMA (50 ng/ml), ionomycin (1 μM) or PMA plus ionomycin for 1 hour. β-Actin was used as loading controls. Data are representative of three independent experiments.

(**d**) HEK293T cells were co-transfected with pNL4-3 and the indicated expression plasmids encoding Regnase-1, Rouqin-1 and Roquin-2. Forty eight hours post-transfection, a TZM-bl reporter assay was performed to measure the production of infectious virus in the cell culture supernatants. Infectious virus yields normalized to the empty vector control are shown as mean values ± s.d. derived from of biological replicates (n = 3). *P* values were calculated using unpaired two-tailed Student's *t*-test. ***P < 0.005.

(**e**) Previously reported MALT1 substrate proteins and their cleavage sites.

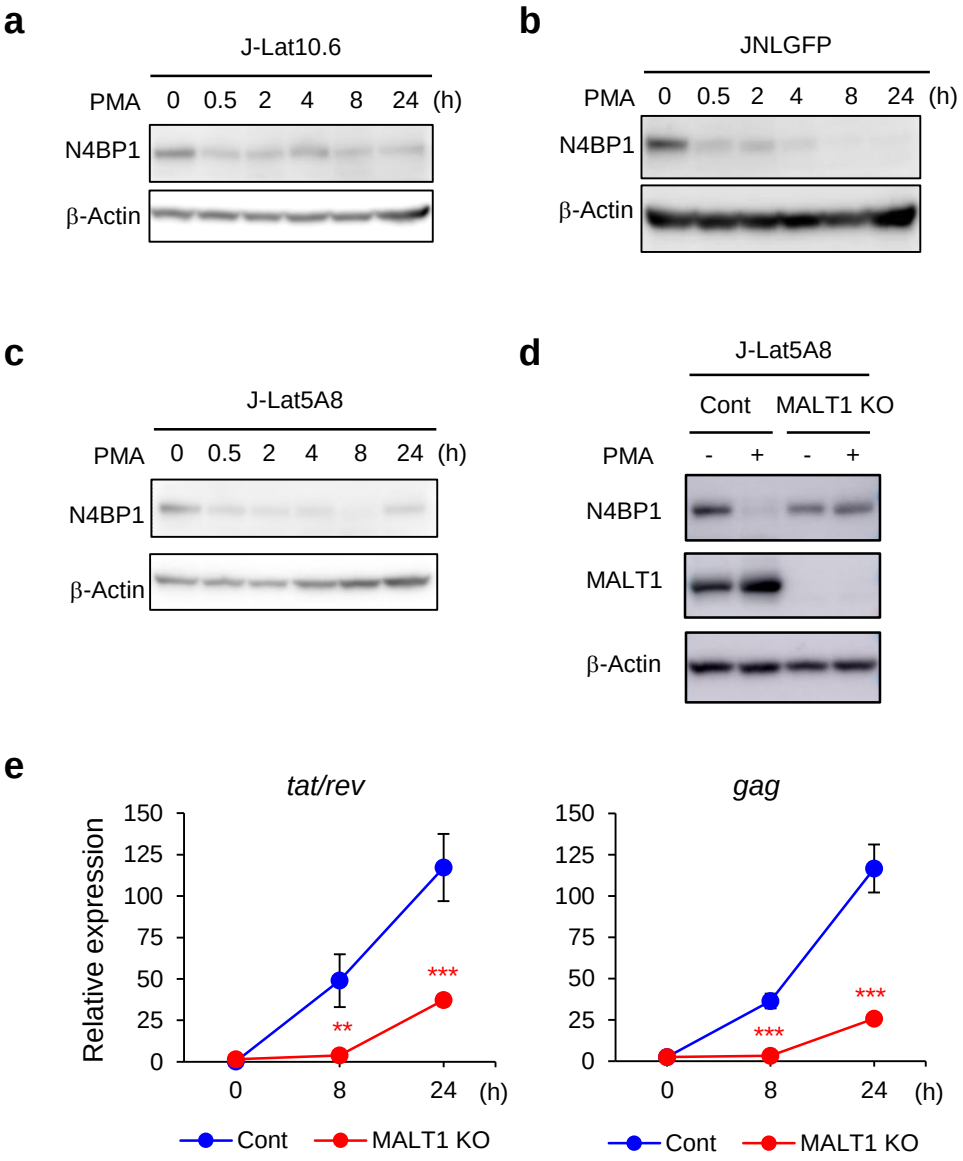

Supplementary Figure 11. MALT1 contributes to viral reactivation in latently infected cells.

(**a**, **b** and **c**) Immunoblot analysis of N4BP1 in cell lysates from J-Lat10.6 (**a**), JNLGFP (**b**) or J-Lat5A8 (**c**) cells stimulated with PMA (50 ng/ml) for the indicated periods of time. β-Actin was used as loading controls. Data are representative of three independent experiments.
(**d**) Immunoblot analysis of N4BP1 and MALT1 in cell lysates from MALT1-deficient or control J-Lat5A8 cells stimulated with PMA (50 ng/ml) for 24 hours. β-Actin was used as loading controls. Data are representative of three independent experiments.
(**e**) Expression of *tat/rev and gag* mRNAs was quantified by qPCR in MALT1-deficient or control J-Lat5A8 cells stimulated with PMA (50 ng/ml) for the indicated periods. Data are shown as mean ± s.d. of biological replicates (n = 3). *P* values were calculated using unpaired two-tailed Student's *t*-test. **P < 0.01; ***P < 0.005.

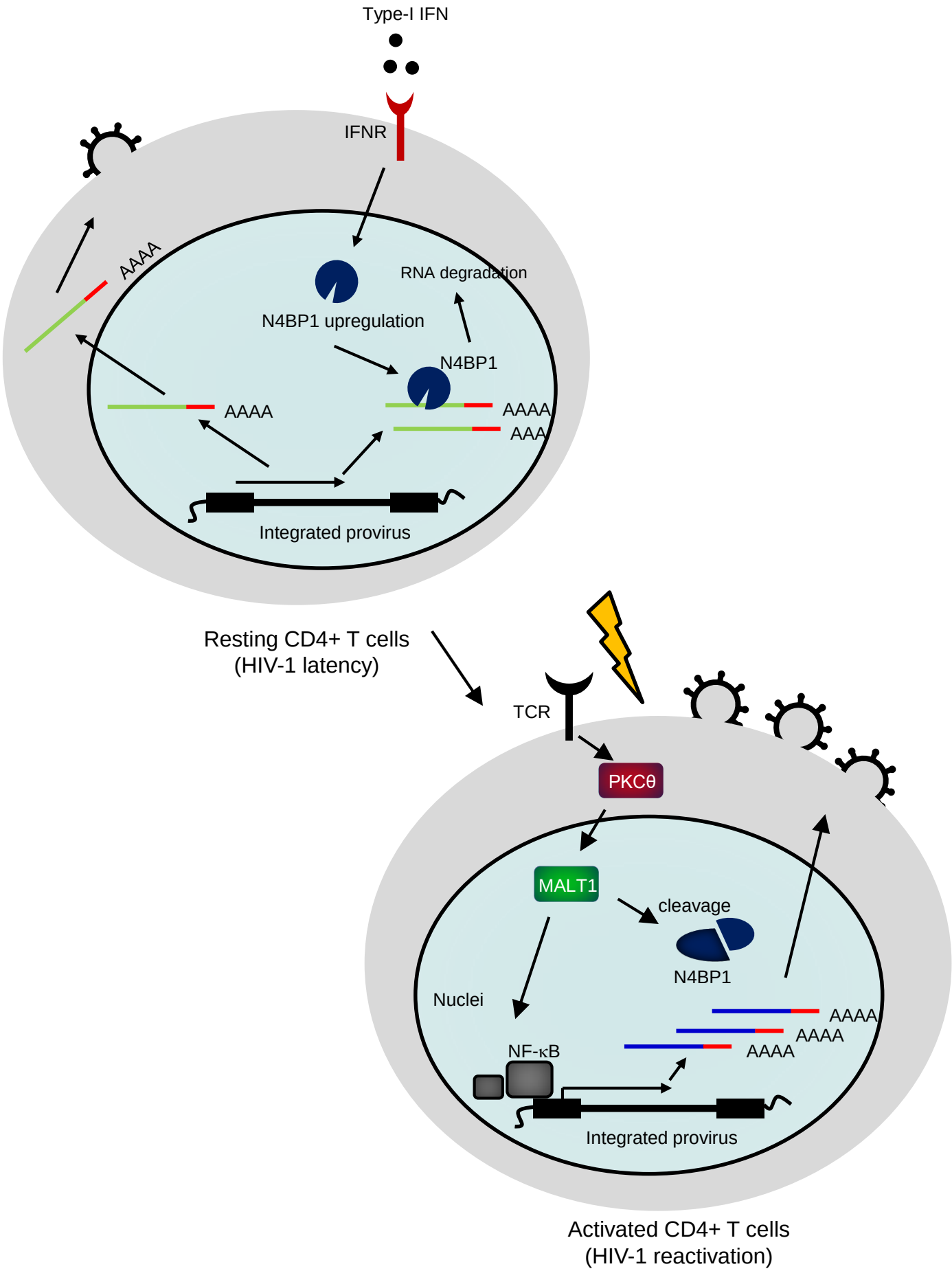

Supplementary Figure 12. Schematic model of the function of N4BP1 in inhibiting HIV-1 infection and its regulation in HIV-1 reactivation.

Supplementary Table 1. Genes used for the screening of proteins harboring RNA binding domains and inhibiting HIV-1 infection.

No	Gene Name	Accession Number		No	Gene Name	Accession Number
1	GPATCH4	BC056904		32	ZC3H7A	BC027330
2	GPATCH2	BC042193		33	IREBP1	BC018103
3	GPATCH2	BC063474		34	ZCCHC17	BC050609
4	FTSJD2	BC031890		35	ZC3H8	BC032001
5	PINX1	BC015479		36	HNRNPC	BC103758
6	KIAA0391	BC032221		37	CPSF4	BC050738
7	RBM5	BC046643		38	CPSF4L	BC004603
8	ZCCHC4	BC016914		39	Zc3h15	BC031845
9	NKRF	BC047878		40	Zc3h14	BC024824
10	GPATCH8	BC019948		41	Zc3h11a	BC005786
11	GPATCH4	BC056904		42	ZFP36L1	BC018340
12	GPATCH3	BC096468		43	TIAL1	BC010496
13	SRRD	BC017682		44	Zc3h18	BC030495
14	RBM10	BC004674		45	HNRNPD	BC011172
15	RBM6	BC026129		46	Zcchc6	BC023880
16	ARFRP1	BC010713		47	Zc3h6	BC043311
17	ARFPR1	BC021513		48	HNRNPK	BC006694
18	ZCCHC9	BC032736		49	N4BP1	BC004022
19	PNPT1	BC027228		50	PCBP3	BC042440
20	QKI	BC019917		51	PCBP4	BC010694
21	ANKHD1	BC040231		52	KHDRBS1	BC002051
22	FXR1	BC019139		53	RNF141	BC018104
23	TARDBP	BC071657		54	RNF11	BC020964
24	YTHDC1	BC053863		55	RNF32	BC015416
25	YTHDC1	BC041119		56	PCBP2	BC107688
26	RIG-I	BC015946		57	RNF7	BC008627
27	FUBP1	BC014763		58	RNF138	BC018107
28	ZCCHC7	BC036940		59	RNF6	BC034688
29	ZCCHC11	BC048301		60	IGF2BP3	BC065269
30	ZCCHC18	BC017627,		61	RNF213	BC032220
31	ZC3H7A	BC046363		62	MEX3b	BC111545

Supplementary Table 2. RT-qPCR Primer Sets

Accession No	Gene	Forward	Reverse
AF324493.2	Tat/Rev	5′-ATGGCAGGAAGAAGCGGAG-3′	5′-ATTCCTTCGGGCCTGTCG-3′
AF324493.2	Gag2	5′-GTGTGGAAAATCTCTAGCAGTGG-3′	5′-CGCTCTCGCACCCATCTC-3′
AF324493.2	Gag3	5′-GTGTGGAAAATCTCTAGCAGTGG -3′	5′-CGCTCTCGCACCCATCTC -3′
AF324493.2	Vif	5′-GGCGACTGGGACAGC -3′	5′-CACACAATCATCACCTGCC -3′
NM_153029.4	N4BP1	5′- CCCGATGATCCTCTGGGAAG -3′	5′- TTTGGCAGGGCACTGAGTAG -3′
NM_004335.4	Tetherin	5′- GTGTCGCAATGTCACCCATC -3′	5′- GGGAAGCCATTAGGGCCATC -3′
NM_002176.4	IFN-β	5′- TTGTTGAGAACCTCCTGGCT -3′	5′- TGACTATGGTCCAGGCACAG -3′
X03205.1	18S	5′- CGGACAGGATTGACAGATTG -3′	5′- CAAATCGCTCCACCAAGTAA -3′
NM_005101.4	ISG15	5′- ACTCATCTTTGCCAGTACAGGAG -3′	5′- CAGCATCTTCACCGTCAGGTC -3′
NC_002017.1	Influenza A (segment 4; HA)	5′- GGCCCAACCACAACACAACC -3	5′- AGCCCTCCTTCTCCGTCAGC -3
AF324493.2	HIV-1 Total	5′- CCTCAGATGCTGCATATAAG -3	5′- CAGGCTCAGATCTGGTCTAA -3
NC_001501	MLV gag	5′- GTCTGAGAATATGGGCCAGA -3	5′- CTTGATCTTAACCTGGGTGA-3
X52154.1	SIVcpz*Ptt*	5′- ACATCTAGTATGGGCCGGAA -3	5′- TTCTGGAGAACCAATGTCTACC -3′
Y07723.1	HFV gag	5′- ACTTGATGTTGAAGCTCTGG -3′	5′- ATCCTTCAGTAAGGCGAAGA -3′
NM_001256799.2 NM_001289745.2 NM_001289746.1 NM_001357943.1 NM_002046.7	GAPDH	5′- GTTGCCATCAATGACCCCTTCATTGACC -3′	5′- CAGCATCGCCCCACTTGATTTTGG -3′
NM_001101.5	ACTB	5′- GCGAGAAGATGACCCAGATC -3′	5′- CCAGTGGTACGGCCAGAGG -3′
NM_000194.3	HPRT1	5′- TATGGCGACCCGCAGCCCT -3′	5′- CATCTCGAGCAAGACGTTCAG -3′
NM_000633.2 NM_000657.2	BCL2	5′- TCCCTCGCTGCACAAATACTC -3′	5′- ACGACCCGATGGCCATAGA -3′
NM_001354870.1 NM_002467.6	cMYC	5′- GCGTCCTGGGAAGGGAGATCCGGAGC -3′	5′- TTGAGGGGCATCGTCGCGGGAGGC TG -3′
NM_001261.3	CDK9	5′- ATGGCAAAGCAGTACGACTCG -3′	5′- GCAAGGCTGTAATGGGGAAC -3′
NM_001240.4	CCNT1	5′- ACAACAAACGGTGGTATTTCACT -3′	5′- CCTGCTGGCGATAAGAAAGTT -3′

NM_001277842.1			
NM_001290230.1 NM_001798.5 NM_052827.3	CDK2	5′- TTTGCTGAGATGGTGACTCG -3′	5′- CTTCATCCAGGGGAGGTACA -3′
NM_001330384.1 NM_014299.2 NM_058243.2	BDR4	5′- ACCTCCAACCCTAACAAGCC -3′	5′- TTTCCATAGTGTCTTGAGCACC -3′
NM_020529.2	NFKBIA	5′- GAGGAGTACGAGCAGATGGTC -3′	5′- CAGGTTGTTCTGGAAGTTGAG -3′
NM_002190.3	IL17A	5′- CAACCGATCCACCTCACCTT -3′	5′- GGCACTTTGCCTCCCAGAT -3′
NM_020525.5	IL22	5′- GCAGGCTTGACAAGTCCAACT -3′	5′- GCCTCCTTAGCCAGCATGAA -3′

Supplementary Table 3. Sequence used for *in vitro* transcription and *in vitro* cleavage assay (Fig. 4d).

GGTCTCTCTGGTAAGACCAGATCTGAGCCTGGGAGCTCTCTGGCTAACTAGGGAACCCA
CTGCTTAAGCCTCAATAAAGCTTGCCTTGAGTGCTCAAAGTAGTGTGTGCCCGTCTGTTG
TGTGACTCTGGTAACTAGAGATCCCTCAGACCCTTTTAGTCAGTGTGGAAAATCTCTAGC
AGTGGCGCCCGAACAGGGACTTGAAAGCGAAAGTAAAGCCAGAGGAGATCTCTCGACG
CAGGACTCGGCTTGCTGAAGCGCGCACGGCAAGAGGCGAGGGGCGGCGACTGGAAGA
AGCGGAGACAGCGACGAAGAGCTCATCAGAACAGTCAGACTCATCAAGCTTCTCTATCA
AAGCAACCCACCTCCCAATCCCGAGGGGACCCGACAGGCCCGAAGGAATAGAAGAAGA
AGGTGGAGAGAGAGACAGAG

Uncropped Raw Blots

Figure 1b HIV-1 NL4-3

Anti-p24

Anti-Env

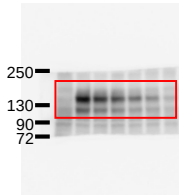

Anti-Flag-N4BP1

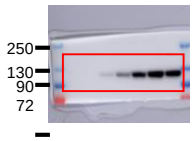

Anti-β-Actin

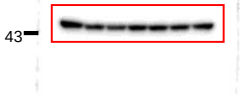

Figure 1b HIV-1 AD17

Anti-p24(cell)

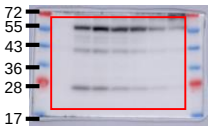

Anti-p24 (sup)

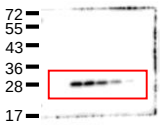

Anti-Flag

Anti-Env

Anti-β-Actin

Figure 2b

Anti-N4BP1

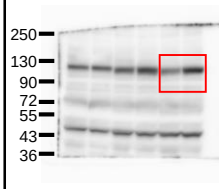

Anti-β-Actin

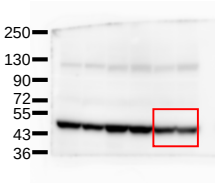

Figure 2f

Anti-N4BP1

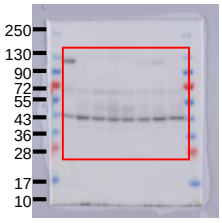

Anti-β-Actin

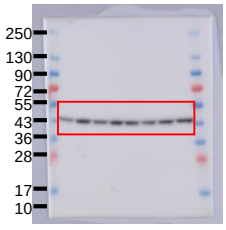

Figure 2g

Anti-N4BP1

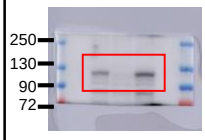

Anti-β-Actin

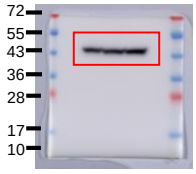

Figure 2h

Anti-Flag

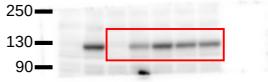

Anti-N4BP1

Anti-β-Actin

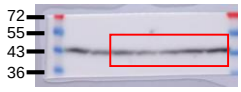

Figure 3b

Anti-N4BP1

Anti-β-Actin

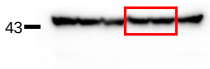

Figure 3d

Anti-N4BP1

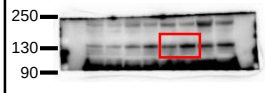

Anti-β-Actin

Figure 3f

Anti-N4BP1

Anti-β-Actin

Figure 4f

HIV-1 RNA probe

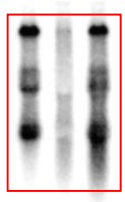

18s

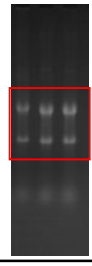

Figure 4h

Figure 4g

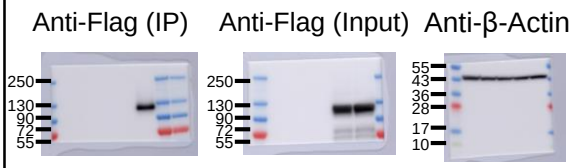

Figure 5a

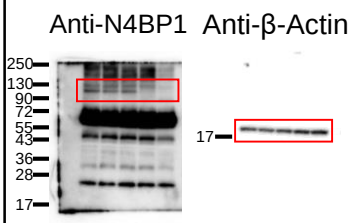

Figure 5b

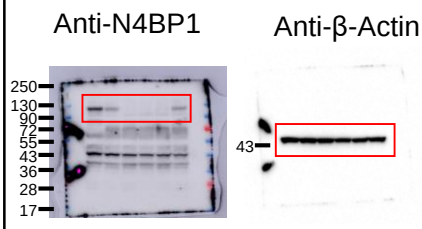

Figure 5c

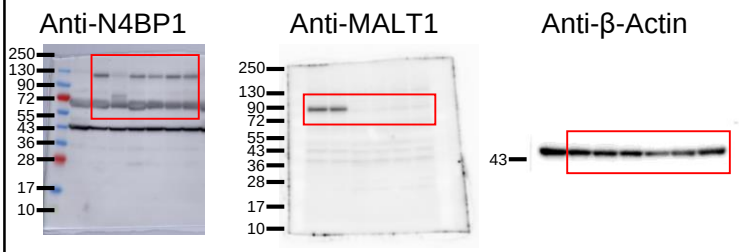

Figure 5d

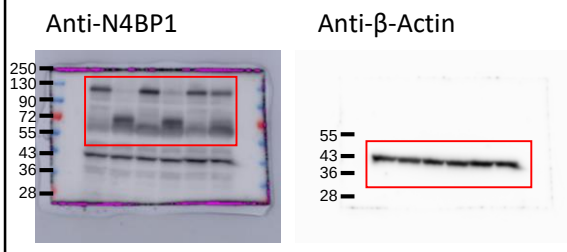

Figure 5f

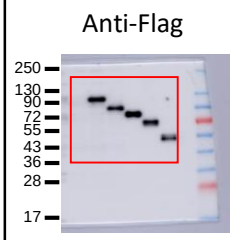

Figure 5i

Figure 5j

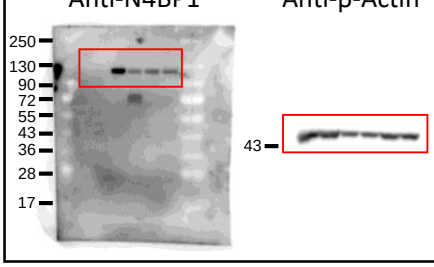

Figure 6a

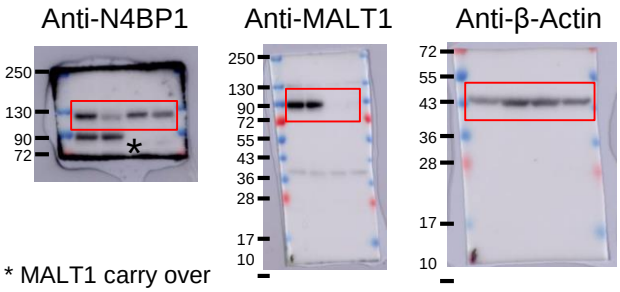

Figure 6b

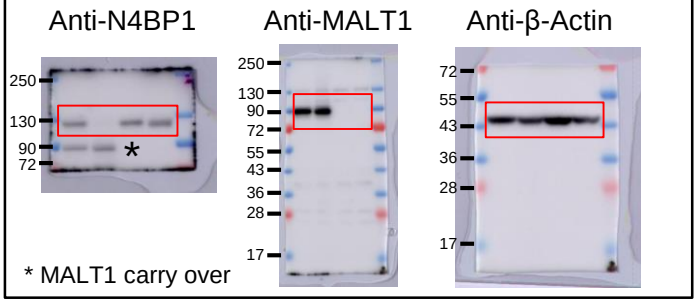

Figure 6e

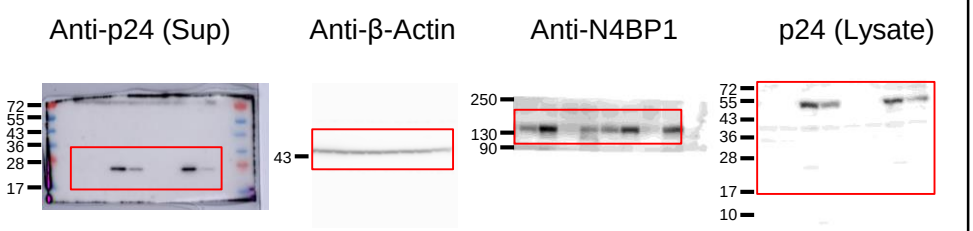

Figure 6f

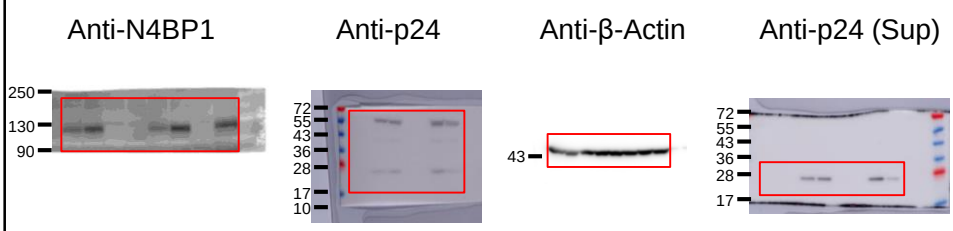

Figure 6g

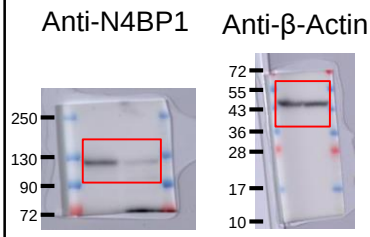

Figure 6h

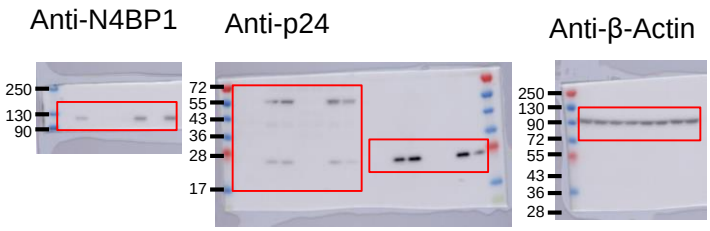

Supplementary Figure 2a

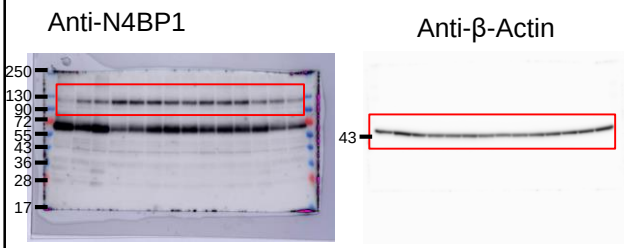

Supplementary Figure 4b

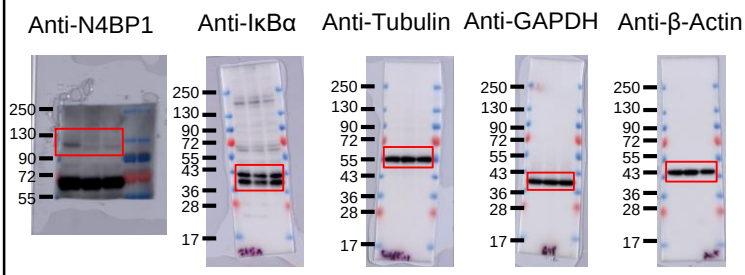

Supplementary Figure 5d

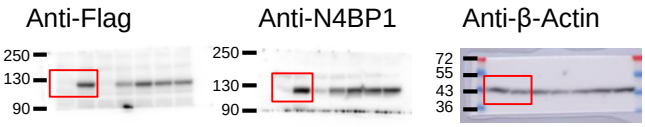

Supplementary Figure 5f

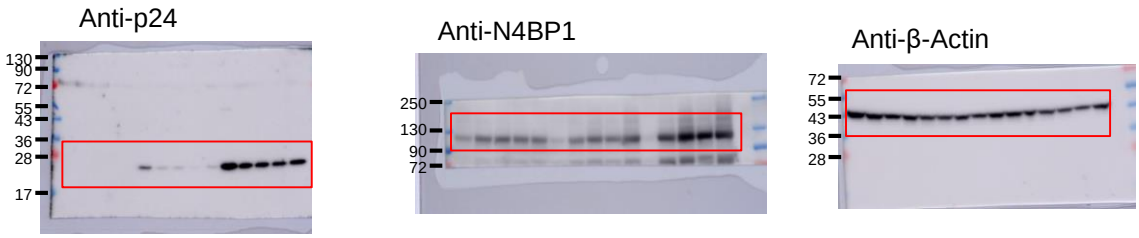

Supplemental Figure 7c

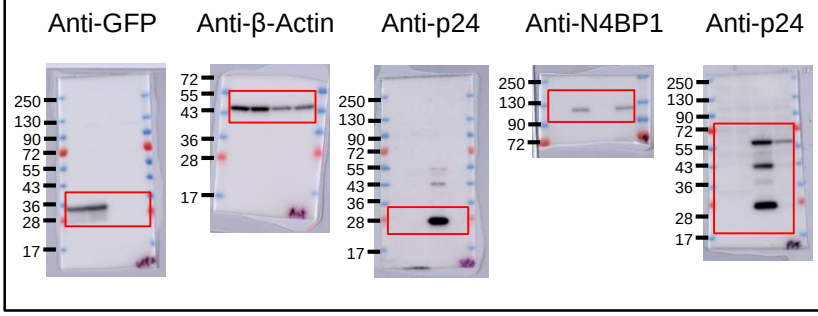

Supplemental Figure 8d

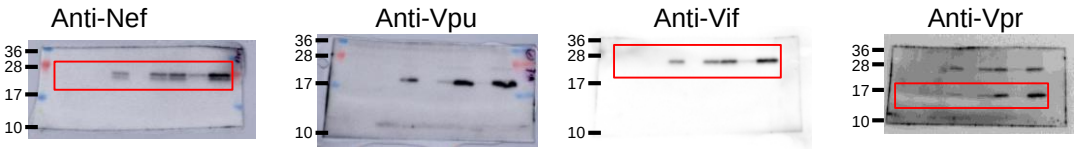

Supplemental Figure 10b

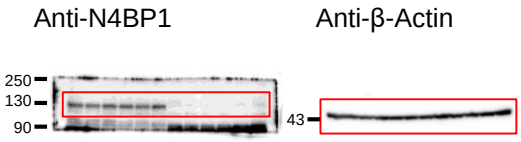

Supplemental Figure 10c

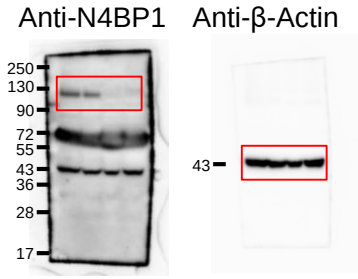

Supplemental Figure 11a

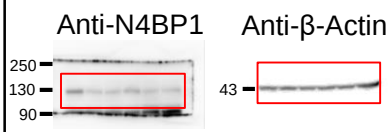

Supplemental Figure 11b

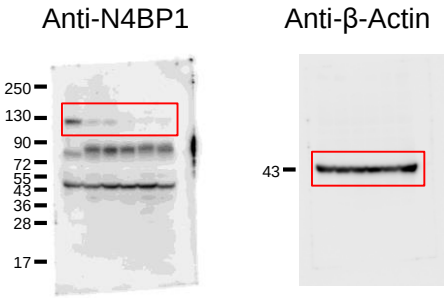

Supplemental Figure 11c

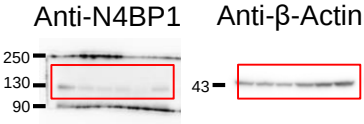

Supplemental Figure 11d

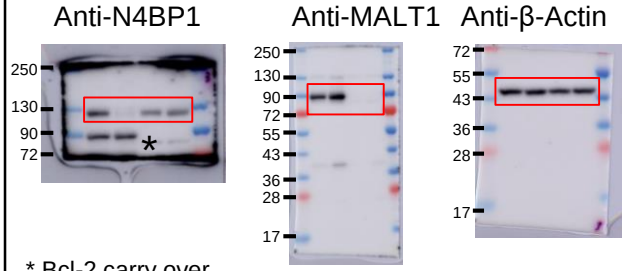

* Bcl-2 carry over